

CANADA - NWT

MINERAL DEVELOPMENT AGREEMENT

POST PILLAR RECOVERY STRATEGIES AT NANISIVIK MINE

PHASE 2 : GROUND STABILITY EVALUATION

S. Vongpalsal, J.E. Udd and G.E. Larocque

MRL 90-27(TR), April 1990

Ph. 2 c. 1

1-11/28



Canmet Information
Centre
D'information de Canmet

MAR 10/94

555, rue Booth ST.
Ottawa, Ontario K1A 0G1

1-1/728

1-1/728 Ph.2c.1
CPUB

POST PILLAR RECOVERY STRATEGIES AT NANISIVIK MINE
PHASE 2 : GROUND STABILITY EVALUATION
S. Vongpalsal, J.E. Udd and G.E. Larocque

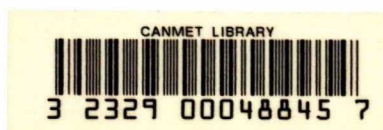
MRL 90-27(TR), April 1990

Ph.2c.1 1-1/728

This project was funded in part by the Canada/NWT Mineral Development Agreement and was conducted under the auspices of CANMET's Mining Research Laboratory.

CANMET Project No. 144610-01-04

CANMET Scientific Authority : R.W.D. Clarke



Ph.2c.1

CPUB.



Energy, Mines and
Resources Canada

Énergie, Mines et
Ressources Canada

CANMET

Canada Centre
for Mineral
and Energy
Technology

Centre canadien
de la technologie
des minéraux
et de l'énergie

POST PILLAR RECOVERY STRATEGIES AT NANISIVIK MINE PHASE 2 : GROUND STABILITY EVALUATION

S. Vongpaisal, J.E. Udd, G.E. Larocque
Mining Research Laboratories, Ottawa, Canada.

April 1990

MINING RESEARCH LABORATORIES
DIVISION REPORT MRL 90-27(TR)

POST PILLAR RECOVERY STRATEGIES AT NANISIVIK MINE

PHASE 2 : GROUND STABILITY EVALUATION

by

S. Vongpaisal* , J.E. Udd**, G.E. Larocque***

ABSTRACT

Under the Northwest Territories Mineral Development Agreement (NWT-MDA), CANMET was subcontracted by Nanisivik Mines Limited, to carry out a technical study to define procedures and strategic mine planning for company consideration in the complete extraction of post pillars. The study by contributing to the safe, productive extension of the mine's life is expected to have a positive socio-economic impact on the Northwest Territories.

This report presents the results of rock mechanics and ground control investigation carried out at Nanisivik Mine as part of the study. The purpose of the present investigation was to evaluate overall ground stability with various pillar extraction options, and to provide related guidelines for strategic mine planning and ground control. The following mining structures and parameters were examined in the investigation, using computer simulations: crown pillar stability, sill pillar stability, pillar mining sequence and stope stability.

The results of this investigation indicate that ground failure is not a significant factor. On the basis of rock mechanics and ground control considerations, the complete removal of post-pillars without backfill should be feasible.

Key words : Post-pillar; Ground stability; Permafrost; Finite element technique.

*Research Scientist, Ph.D., P.Eng.; **Director, Ph.D., P.Eng. ; ***Manager, Canadian Mine Technology Laboratory; Mining Research Laboratories, CANMET, Energy, Mines and Resources Canada, Ottawa,

TECHNIQUES D'EXPLOITATION DES PILIERS À LA MINE NANISIVIK

PHASE 2 : ÉVALUATION DE LA STABILITÉ DU TERRAIN

by

S. Vongpaisal* , J.E. Udd**, G.E. Larocque***

RÉSUMÉ

En vertu de l'Entente sur l'exploitation minérale conclue avec les Territoires du Nord-Ouest, la société Nanisivik Mines Limited a chargé CANMET, par sous-traitance, de réaliser une étude technique de la méthode et des plans stratégiques d'aménagement qu'elle pourrait adopter pour l'extraction complète des piliers de la mine. En contribuant à prolonger la période pendant laquelle la mine pourra être exploitée en toute sécurité, l'étude devrait avoir des incidences socio-économiques positives sur les Territoires du Nord-Ouest.

Ce rapport présente les résultats d'une étude en mécanique des roches et contrôle des pressions de terrain à la mine Nanisivik, réalisée dans le cadre du projet. La présente étude avait pour but d'évaluer la stabilité globale du terrain, selon différentes hypothèses d'extraction des piliers, et de fournir des lignes directrices quant à la planification de la mine et au contrôle des pressions de terrain. Réalisée au moyen de simulations par ordinateur, l'étude a principalement porté sur les structures et paramètres d'extraction suivants: stabilité des stots, stabilité des piliers de niveau, séquence d'extraction des piliers et stabilité du chantier d'abattage.

L'étude démontre que les possibilités de rupture du roc sont limitées et ne constituent pas un handicap lors de l'exploitation. Compte tenu des données sur la mécanique des roches et le contrôle des pressions de terrain, il serait possible d'enlever complètement les piliers sans faire de remblayage.

Mots-clés : pilier; stabilité du terrain; pergélisol; technique des éléments finis.

*Chercheur scientifique, Ph.D., Ing.; **Directeur, Ph.D., Ing.; ***Gestionnaire, Laboratoires canadiens de technologie minière; Laboratoires de recherche minière, CANMET, Énergie, Mines et Ressources Canada, Ottawa,

CONTENTS

	<u>Page</u>
ABSTRACT	i
RÉSUMÉ	ii
1. INTRODUCTION	1
2. BACKGROUND	1
2.1 Geology	1
2.2 Rock Mass Characteristics	2
2.3 Mining Operations	3
3. COMPUTER SIMULATIONS	6
3.1 Assumption	6
3.2 Finite Element Models	7
3.3 Results	7
3.3.1 Stability of Crown Pillar	7
3.3.2 Stability of Sill Pillar	9
3.3.3 Pillar Mining Sequences	9
3.3.4 Stability of Stopes	11
4. GROUND CONTROL	11
5. OBSERVATIONS	12
6. ACKNOWLEDGEMENT	14
7. REFERENCES	14
APPENDIX A - Figures	15

List of Tables

1. Summary of mine rock properties from laboratory tests	4
2. In situ deformation moduli from dilatometer measurements	5
2. Input rock properties for modelling	7

List of Figures

1. Location of Nanisivik Mine, Baffin Island, N.W.T.	16
2. Topographical Map, Main Ore Zone, Nanisivik Mine	17
3. Geology Map, Nanisivik Ore Bodies	18
4. Finite Element Model 1, Variations of Crown Pillar Thickness	19
5. Finite Element Model 2, Cross-section 19250E	20
6. Finite Element Model 3, Cross-section 17800E	21
7. Relaxation Zones, Model 2, Section 19250E, Worst Condition	22

8. Potential Failure Zones, Model 2, Section 19250E, Worst Condition	23
9. Relaxation Zones, Model3, Section 17800E, Worst Condition	24
10. Potential Failure Zones, Model3, Section 17800E, Worst Condition	25
11. Sketch of Pillar Layout, Model 2, Section 19250E	26
12. Sketch of Pillar Layout, Model 3, Section 17800E	27
13. Relaxation Zones, Model 2, Section 19250E, Present Mining Stage	28
14. Relaxation Zones, Model 2, Section 19250E, P1 Mined	29
15. Relaxation Zones, Model 2, Section 19250E, P3 Mined	30
16. Relaxation Zones, Model 2, Section 19250E, P2 Mined	31
17. Relaxation Zones, Model 2, Section 19250E, P1, P3 Mined	32
18. Relaxation Zones, Model 2, Section 19250E, P1, P2 Mined	33
19. Relaxation Zones, Model 2, Section 19250E, P2, P3 Mined	34
20. Relaxation Zones, Model 2, Section 19250E, P1, P2, P3 Mined	35
21. Relaxation Zones, Model 2, Section 19250E, P1, P2, P3, P4 Mined	36
22. Relaxation Zones, Model 2, Section 19250E, P2, P4 Mined	37
23. Relaxation Zones, Model 2, Section 19250E, P1, P2, P4 Mined	38
24. Relaxation Zones, Model 2, Section 19250E, P2, P3, P4 Mined	39
25. Relaxation Zones, Model 3, Section 17800E, Present Mining Stage	40
26. Relaxation Zones, Model 3, Section 17800E, P1 Mined	41
27. Relaxation Zones, Model 3, Section 17800E, P2 Mined	42
28. Relaxation Zones, Model 3, Section 17800E, P1, P2 Mined	43
29. Excavation Displacements At Stope Roof, Model 2, Section 19250E	44
30. Excavation Displacements At Stope Roof, Model 2, Section 19250E	45
31. Excavation Displacements At Stope Roof, Model 2, Section 19250E	46
32. Excavation Displacements At Stope Roof, Model 2, Section 19250E	47
33. Excavation Displacements At Stope Roof, Model 3, Section 17800E	48
A1. Major Principal Stress Distributions, Model 1	49
A2. Minor Principal Stress Distributions, Model 1	50
A3. Drucker-Prager Safety Factor Plots, Model 1	51

1. INTRODUCTION

Under the Northwest Territories Mineral Development Agreement (NWT-MDA), CANMET was subcontracted by Nanisivik Mines Limited, to carry out a technical study to define procedures and strategic mine planning for company consideration in the complete extraction of post pillars. The study by contributing to the safe, productive extension of the mine's life is expected to have a positive socio-economic impact on the Northwest Territories.

This report presents the results of rock mechanics and ground control investigation carried out at Nanisivik Mine as part of the study. The purpose of the present investigation was to evaluate overall ground stability with various pillar extraction options, and to provide related guidelines for strategic mine planning and ground control. The following mining structures and parameters were examined in the investigation:

1. Crown pillar stability.
2. Sill pillar stability.
3. Pillar mining sequences.
4. Stope stability.

Visits were made to the property to collect information and to hold technical discussions with mining personnel. Final assessments were based on the use of finite element computer simulations combined with engineering judgement.

2. BACKGROUND

The following is a brief summary of the information gathered for the purpose of carrying out the investigation.

2.1 Geology(1,2)

The Nanisivik Mine is located near the north end of Baffin Island, Northwest Territories. The latitude and longitude of the site are 70° 08' N and 80° 25' W respectively (see Figure 1).

The Nanisivik ore body consists of sphalerite and galena in a pyrite matrix. Minor amounts of silver are found associated with the sphalerite. The host rocks are dolomites of the Society Cliffs Formation. The colour of the dolomite varies from light grey to

almost black. Pyrite is the main mineral, but in places other sulphides are present in ore-grade proportions.

The main ore body occurs in the permafrost zone at a depth of 20 to 130 m below surface with a horizontal extent of 3 000 m. The mine is entirely within the permafrost zone, which extends to a depth of 600 m below surface. The general strike of the main ore zone is EW and the dip is approximately 15° NNW. The average width of the main ore zone is 100 m with a thickness varying from 0 to 20 m. Figure 2 shows the topographical map of the main ore zone. Sulphides occur below the main lenses, either as horizontal lenses or as near-vertical vein-like structures. It appears that the sulphide occurrences do not have any direct relationship to brecciation, marmorization, or lithological changes within the Society Cliffs Formation.

Major discontinuities of the Nanisivik ore bodies are shown in Figure 3. A study of Figure 3 indicates that the sulphide bodies cut across some major faults, with little or no change in elevation, and cut horizontally across bedding planes in the dolomite.

Major joint dips are almost vertical, with a general strike of 142° or $S38^{\circ}E$. A minor jointing system strikes $N55^{\circ}E$, with a vertical dip.

Jointing does not appear in the sulphide zones.

2.2 Rock Mass Characteristics

Rock mass characterizations to establish the setting of the Nanisivik Mine were carried out by CANMET in field and laboratory investigations which involved the following tests:

1. TV Borehole inspections.
2. Dilatometer tests.
3. Ground stress determinations.
4. Ground movement monitoring.
5. Determination of the mechanical properties of mine rocks.

Details of the investigations are presented in a Phase 1 report (3). The main conclusions are presented below:

1. The host rock is strong and massive. Inspection of roof strata up to 6.6 m above the roof line indicated sound roof conditions except for minor blast damage close to the roof line and some minor fracturing near the portal.

2. Ground stress determinations in the dolomite of the south abutment showed the maximum stress is oriented NE-SW in the horizontal plane with an average magnitude of 4.5 MPa. The maximum ratio of horizontal to vertical stress is 3.2:1. The magnitude of the vertical stress is equivalent to overburden stress.
3. Dolomite and sulphide behaved elastically. Table 1 summarizes laboratory test results. Table 2 provides the in situ elastic moduli of rocks determined from dilatometer measurements.

2.3 Mining Operations

Room-and-pillar mining is employed to extract the Nanisivik orebody at a production rate of about 2400 tonnes/day. It is one of Canada's largest and most efficient room-and-pillar operations. The pillars are spaced on a 25×25 m pattern with an average cross-section area of 64 m^2 ; pillar height varies from 5 to 20 m. An extraction of 75% has been achieved in the main ore zone. Thus, approximately 800 000 tonnes of ore grading at 10.5% Zn, 0.7% Pb, and 54 gm/tonne Ag is committed to 350 post-pillars thought to be required for stabilization of the back.

All underground drilling is dry and entails dust collectors mounted on the drills. Dry drilling is necessary because the mine is in permafrost. The year round temperature is from -10^0 to -12^0 C.

The hole-spacing pattern is 1×1 m for drift and slash rounds, and 1 m high \times 1.2 m wide for bench rounds.

All blasting is done with ANFO with Nonels, B-line and electrical detonators as accessories. Powder factors vary from 0.3 to 0.6 kg per tonne.

Ore is hauled to ore passes by DJB 330 rear-dump and Wagner M439 haulage trucks. Truck loading is done with Caterpillar 980 loaders and Wagner ST 8 Scooptrams. Other equipment used in the mine includes: Eimco Jarvis Clark RBM 11 rock-bolters; a Jarvis Clark scissor lift truck/giraffe; a Jarvis Clark ANM 12 ANFO truck; an Atlas Copco Diamec 250 diamond drill; and a Caterpillar 1406 grader.

Table 1 - Summary of Mine Rock Properties from Laboratory Tests

Test No.	Rock Type (Test Site)	Hgt (mm)	Dia. (mm)	Ratio H/D	E (GPa)	v	UCS (MPa00)	Failure Load (KN)	Testing Method
NML-SA1	Dolomite	345	137	2.53	57.03	0.26	82.13	1320	Uniaxial compression
NML-SA2	(Site B)	343	137	2.50	53.17	0.23	128.70	1921	Uniaxial compression
NML-SA3	(Site B)	302	137	2.20	64.07	0.24	153.37	2290	Uniaxial compression
NML-SA4	(Site B)	295	137	2.15	50.50	0.22	89.40	1355	Uniaxial compression
NML-AO5	(Site B)	341	137	2.49	43.93	0.20	73.70	1100	Uniaxial compression
NML-AO6	(Site B)	-	137	-	42.41	0.23	-	-	Radial compression*
NML-P10	Sulphide (pillar)	315	137	2.30	32.42	0.30	42.00	627	Uniaxial compression
NML-NA1	Sulphide	129	53	2.43	74.23	0.18	75.17	178	Uniaxial compression
NML-NA2	+ quartz	134	53	2.53	64.82	0.12	112.75	267	Uniaxial compression
NML-NA3	Stringers (Site A)	132	53	2.50	58.55	0.15	80.10	190	Uniaxial compression
NML-EX	Dolomite (Site B)	-	23	-	Mean Value: (27 tests)		141,30 ±23.8	-	Point load test**

Note: Elastic modulus and Poisson's ratio obtained at 20 to 56% of failure load.

Uniaxial compressive strength of 137 mm diameter and 53 mm diameter core specimens were determined using 2000 Ton and 60 Ton press, respectively (1 kN = 224.82 lbs).

(*) Values obtained from strain readings of axial and circumferential gauges of CSIR strain cells when overcored hollow core cylinder are radially loaded using a Hoek cell.

(**) BEMEK - portable rock tester used.

Table 2 - In situ deformation moduli from dilatometer measurements

Location	Rock Type	Test No.	Depth from Collar (m)	In situ Deformation Modulus (GPa)	Remarks
Site A	Sulphide	NQ4-1	1.55	22.60	
	Sulphide	NQ4-2	2.50	19.90	
	Sulphide	NQ4-3	5.25	21.80	
Site C	Dolomite	NQ3-1	1.50	-	Test not successful
	Dolomite	NQ3-2	1.50	-	Test not successful
	Dolomite	NQ3-3	1.50	60.68	----
	Dolomite	NQ3-4	2.50	-	Test not successful

Note: Deformation modulus value, E , is calculated based on the solution for an isotropic linear elastic thick hollow cylinder as follows:

$$E = 2(1 + \nu) (V_o + V_m) \frac{1}{\frac{\Delta V}{P_b} - C}$$

where, ν = Poisson's ratio

V_o = initial volume of the dilatable membrane, (deflated probe).

V_m = mean volume injected into the probe.

$\Delta V = V_1 - V_2$, the difference between injected volumes corresponding to two points on the linear portion of the loading curve.

$\Delta P_b = 0.955 (P_1 - P_2)$: $P_1 - P_2$ is the difference in pressure between two corresponding points on the loading curve and 0.955 is the pressure connection factor.

$C = a - b$, where "C" is the correction factor for compressibility of the dilatable membrane, "a" is a volume/pressure relationship from calibrating the probe in a steel cylinder, and "b" is the stiffness of the cylinder in terms of volume/pressure.

3. COMPUTER SIMULATIONS

In this study, finite element computer simulations were carried out to estimate overall mine stability. The finite element technique is well known as a powerful tool for stress and displacement analysis. It has been successfully applied in mine design and planning worldwide .

3.1 Assumption

The assumptions made in carrying out the investigation's computer simulations and analysis were the following:

1. The static two-dimensional plane strain model is applicable. It permits simulation of a greater variety of rock types and mining geometries than is possible with alternative methods. It is, as well, the most economic method of carrying out mine stability evaluations and provides a valid but conservative simulation of the actual conditions. Three-dimensional modelling would be much more expensive;
2. The materials being modelled can be considered homogeneous, linear elastic, and isotropic. This assumption is considered valid to a first approximation under the hard rock mining conditions being simulated. Table 3 provides the input parameters used in this study;
3. In situ stress magnitudes are linearly related to depth, and the horizontal principal stress components are 3 and 0.7 times, respectively, the vertical stress component. These magnitudes are inferred from the in situ stress determination and are representative of stress conditions generally encountered in the Canadian Shield;
4. Mine openings are instantly excavated without filling; and
5. Maximum tension and Mohr-Coulomb, using Drucker-Prager equations, provide valid failure criteria.

Table 3 Input rock properties for modelling

Rock type	Specific gravity	Modulus of elasticity (MPa)	Poisson's ratio	Cohesive strength (MPa)	Internal angle of friction (degrees)
Dolomite	2.8	26000	0.20	6	30
Sulphide	4.0	29000	0.18	5	30

3.2 Finite Element Models

A series of computer simulations using three major finite element models were carried out to examine stress conditions around mine openings. Details of the models are provided below:

Model 1 : This model was constructed to examine crown pillar stabilities and ground reactions to mine openings. (see Figure 4).

Model 2 : This model was constructed along 19250E section. This section was chosen because it represents the area with the most potential for ground problems, i.e., where the crown pillar is thinnest. The purpose was to examine stope stability and ground reaction to the extraction of various 10 m high pillars and to compare the results obtained from computer simulations with those obtained from rock mechanics instrumentation. (see Figure 5).

Model 3 : This model was constructed along 17800E section, an area with the tallest post pillars. The purpose was to examine stope stability and ground reaction with extraction of various 20 m high pillars. (see Figure 6).

3.3 RESULTS

In this investigation, the relaxation zone is considered to be defined by the presence of either major or minor principal tensile stresses. A high tensile zone is defined as a zone where tensile stresses exceed 1 MPa.

3.3.1 Stability of Crown Pillar

Model 1 was used to examine stresses and ground conditions in the crown pillar and neighbouring stopes. A parametric study was made to examine the impact of crown pillar thickness and stope span on the relaxation zone created. Sensitivity analysis was carried out to determine the influence of the cohesive strength and angle of internal

friction of the dolomite on the failure zone. In this study, crown pillar thickness was varied from 20 to 140 m. To be representative of a typical mine stope geometry, a ratio of stope height to span of 1:10 was used.

Figures A1 to A3 are typical stress distributions and Drucker-Prager safety plots for the immediate areas around stopes.

The conclusions drawn from Model 1 simulations are the following:

1. No significant potential failure zones are indicated in the crown pillar. Thus, the simulation indicates that the crown pillar should be stable.
2. The relaxation zone extends to the surface when the ratio of crown pillar thickness to stope span is less than 1:2.
3. When the ratio of crown pillar thickness to stope span is greater than 1:2, the relationship between relaxation zone and crown pillar thickness can be expressed as follow:

$$H_r/S = 0.48 - 0.23T_c/S \quad (1)$$

where:

H_r = height of relaxation zone

S = stope span

T_c = crown pillar thickness

4. The potential failure zone varies inversely with the dolomite's cohesion. Its height can be expressed by the following relationship:

$$H_f = 130.76 - 51.33C_0 + 6.55C_0^2 - 0.27C_0^3 \quad (2)$$

where:

H_f = height of potential failure zone (m).

C_0 = cohesive strength of dolomite (MPa).

The above engineering equations provide guidelines for ground control and ground reinforcement design. The equations are valid for the range of values within the parameters assumed.

3.3.2 Stability of Sill Pillar

Models 2 and 3 were used to assess the structural stability of the sill pillar located between the main ore zone and the lower lenses. It was assumed that both ore zones were completely mined in order to simulate the worst possible condition. Figures 7 to 10 show relaxation and potential failure zones around the mine openings.

The main conclusions drawn from the results of these mine model simulations are:

1. No significant potential failure zones are indicated in the sill pillars under this worst case condition. The sill pillars are considered to be stable.
2. Potential failure zones are indicated in the sill pillars at the distance between the corner of stope walls and $\frac{1}{4}$ of pillar span, and extend diagonally towards the centre of the pillar.
3. In Model 2, a large high tensile stress zone occurs in the north side abutment of the main ore zone and the lower ore lenses. The tensile stresses combined with major discontinuities would indicate the sill pillar could pose major ground failure problems.

3.3.3 Pillar Mining Sequences

The influence of pillar mining sequence on ground stability was examined using Models 2 and 3. Twelve cases were simulated using Model 2 and four using Model 3. The following summarizes the cases studied:

Model 2: (see Fig. 11)

1. Present mining stage.
2. P1 mined.
3. P3 mined.
4. P2 mined.
5. P1 and P3 mined.
6. P1 and P2 mined.
7. P2 and P3 mined.
8. P1, P2, and P3 mined.
9. P1, P2, P3, and P4 mined.
10. P2 and P4 mined.
11. P1, P2, and P4 mined.
12. P2, P3 and P4 mined.

Model 3: (see Fig. 12)

1. Present mining stage.
2. P1 mined.
3. P2 mined.
4. P1 and P2 mined.

Figures 13 to 28 show the relaxation zones realized around the stopes for the case studied.

The main conclusions drawn from the simulations are the following:

1. Model 2 studies indicate that, at the present mining stage, central pillars are likely to carry higher loads than side pillars. The average central pillar stress is 6 MPa, whilst the average north and south side pillar stresses are 4.3 and 4.5 MPa, respectively.
2. Model 3 studies indicate that, at the present mining stage, side pillars are likely to carry higher loads than the central pillars. The average side pillar and central pillar stresses are 6.5 and 5 MPa, respectively.
3. Model 2 studies also indicate that, when the thickness of the north abutment is less than twice the stope width, the best pillar mining sequence in terms of stability is to mine the south side pillar first, the north side pillar second and the central pillar last. With this sequence pillar loads and potential ground failure zones induced by mining stresses are minimized. Post-pillars in the main ore zone should be completely extracted before completely mining post-pillars in the lower lenses.
4. Similarly, Model 3 studies indicate that when the thickness of the abutments is greater than 2 times the stope width the optimum pillar extraction sequence is removal of the central pillar first followed by removal of the north side and south side pillars. Due to symmetry the model does not indicate an order of preference.
5. In general, high tensile stress zones occur near the surface pillars (about 1 m deep) at locations adjacent to the floor and the roof horizons of the stopes. Consequently, some localized ground spalling or tensile cracks may be developed at these locations. These surface effects are not a cause for major concern with respect to pillar instability

unless major discontinuities or poor ground zones pass through these high tensile stress zones.

3.3.4 Stability of Stopes

The main conclusions based on the results of Models 2 and 3 computer simulations are the following:

1. No significant potential failure zone is indicated in a stope when all of the post-pillars are extracted. The stope is considered to be stable.
2. Small potential surface failure zones, extending to a depth of 2 m in stope roofs, are developed with pillar extraction.
3. Model 2 studies indicate that potential failure zones in the roof and wall of the north abutment, extending to a depth of 3 m, are developed when post-pillars in the main ore zone are completely mined. (see Figure 20).
4. Model 3 studies indicate that potential failure zones near the roof corners, extending to a depth of 2 m, are developed when post-pillars in the main ore zone are completely mined. (see Figure 28).
5. A maximum excavation displacement of the roof of about 12 mm occurs near the south central portion of the stope when the pillars are completely mined. The roof near the north abutment tends to move upwards about 2 mm. (see Figure 29).

Figures 30 to 33 provide information on estimated roof displacements accompanying excavation from modelling for use in assessing field measurement data.

4. GROUND CONTROL

It is essential that the conclusions reached in this study, based on geotechnical data and numerical analyses, be confirmed by site-specific monitoring studies. Undetected localized discontinuities not allowed for in the analysis could seriously compromise the conclusions reached. Based on the validity of the computer simulation studies the following are given as general guidelines for mine planners and rock mechanics engineers:

1. The high tensile zones which are shown in Figures 13 to 28 should be considered for ground reinforcement in order to minimize ground failure or dilution. A system of 3 m long split sets, installed on a

- 1.2×1.2 m pattern, is recommended for the ground support required in the roof and north wall abutment.
2. Wire screen or straps should be used in localized conditions of poor ground.
 3. The geological structural features should be mapped as accurately as possible for use in establishing ground control and ground support requirements.
 4. The upper sections of pillars should be blasted carefully in order to minimize roof damage. This has the potential of causing ground stability problems. Pre-splitting should be used, if feasible.

5. OBSERVATIONS

Based on the results of this investigation, the following observations are made:

1. The study of strategic post-pillar extraction, simulated in Models 1 to 3, indicates that ground failure should not be a significant factor. On the basis of rock mechanics and ground control considerations, the complete removal of post-pillars without backfill should be feasible.
2. The crown pillar is considered stable. Engineering equations 1 and 2 are provided as a guide to achieve ground control and provide necessary ground support in its design.
3. The sill pillar between the main ore zone and the lower lens is considered to be stable. However, ground conditions and major discontinuities should be carefully observed, especially in the areas measured from the stope corner to $\frac{1}{4}$ of pillar span where high tensile stresses are developed and additional ground control measures might be required. The synergistic effect of high tensile stresses and poor ground conditions or major discontinuities could cause sill pillar stability problems.
4. When the thickness of the north abutment is less than twice the stope width, the best pillar mining sequence is the following: mine the south side pillar first, then the north side pillar and the central pillar last. This sequence should minimize pillar loads and the extent of potential ground failure zones, especially in the eastern portion of the main ore zone.

5. When the thickness of an abutment is greater than twice the stope width, especially in the central portion of the main ore zone, the best pillar mining sequence is the following: mine the central pillar first followed by the north or south pillar. Due to symmetry the model does not indicate an order of preference.
6. From the point of view of access and ground control, post-pillar extraction should be started from the extreme east end of the main ore zone and retreat towards the west.
7. Careful blasting procedures should be used near the tops of pillar to minimize roof damage and to maintain ground stability. Pre-splitting techniques should be attempted, if possible. Pre-splitting near the roof line may be difficult especially in the case of high pillars (about 20 m), and some consideration should be given to the use of the Alimac drilling technique.
8. In the eastern portion of the main ore zone stopes near the north abutment are more prone to failure than stopes near the south abutment. In addition to present ground monitoring systems, MRL rings should be installed in the north abutment to determine stress changes induced by mining during pillar extraction.
9. High tensile zones, which are induced by mining are shown in Figures 13 to 28. If poor ground conditions exist in these zones, artificial ground reinforcement should be used to stabilize stope walls and to minimize dilution. General guidelines for ground control are given in section 4.
10. During pillar extraction ground conditions should be regularly observed and the information fed back to CANMET for use in back analyses, development of a ground control expert system and, if necessary, additional simulations for use by Nanisivik in undertaking design modifications.

6. ACKNOWLEDGEMENTS

Thanks are due to Messrs. G. Clow, Project Co-ordinator; W. McNeil, Mine Manager; P. Hansman, Chief Engineer, Nanisivik Mines Limited; and M. Irving, MDA-Coordinator NWT, for their helpful cooperation in this study project, and to R.W.D. Clarke, Scientific Authority and R. Blake, Business Co-ordinator, CANMET for their valuable suggestions.

7. REFERENCES

1. T. Loree, "Nanisivik: Mine at the top of the world"; The Northern Miner Magazine, February 1989.
 2. J.C. Moormann, "Pillar recovery at Nanisivik"; Nanisivik Mines Limited; Internal Report; 1980.
 3. B. Arjang and G. Herget, "Post pillar recovery strategies at Nanisivik Mine, Phase 1 : Ground control instrumentation and stress determinations"; Division report, MRL 89-147(TR); CANMET, Energy, Mines and Resources Canada; November 1989.
-

APPENDIX A

Figures

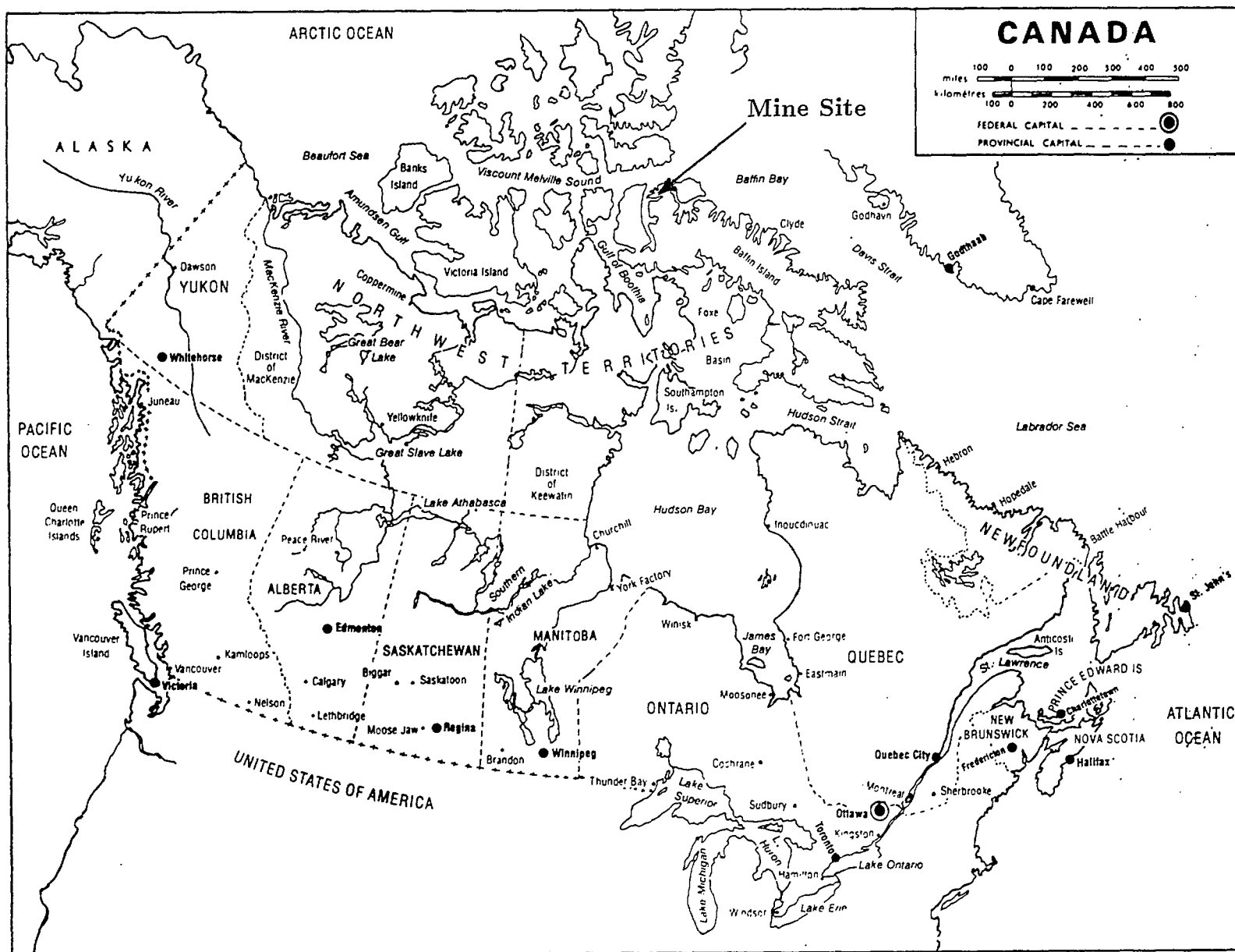


Fig. 1 - Location of Nanisivik Mine, Baffin Island, N.W.T.

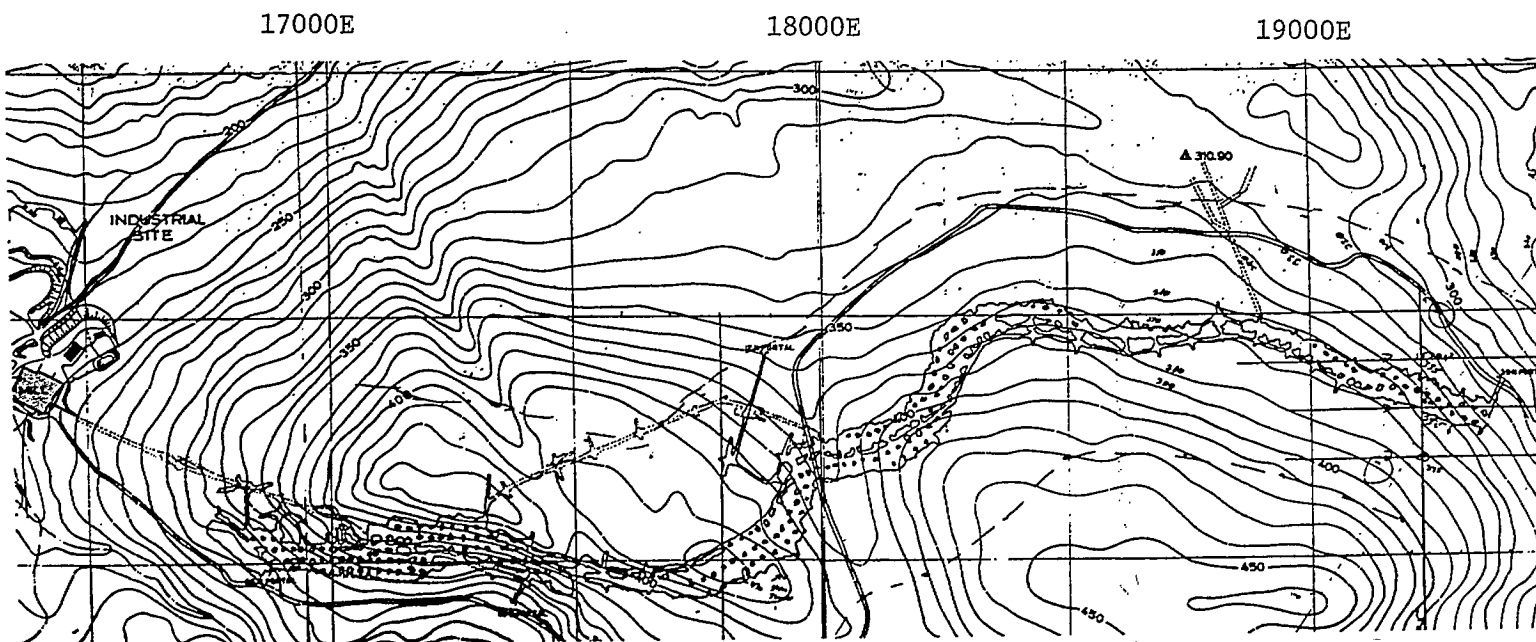


Fig. 2 - Topographical Map, Main Ore Zone, Nanisivik Mine

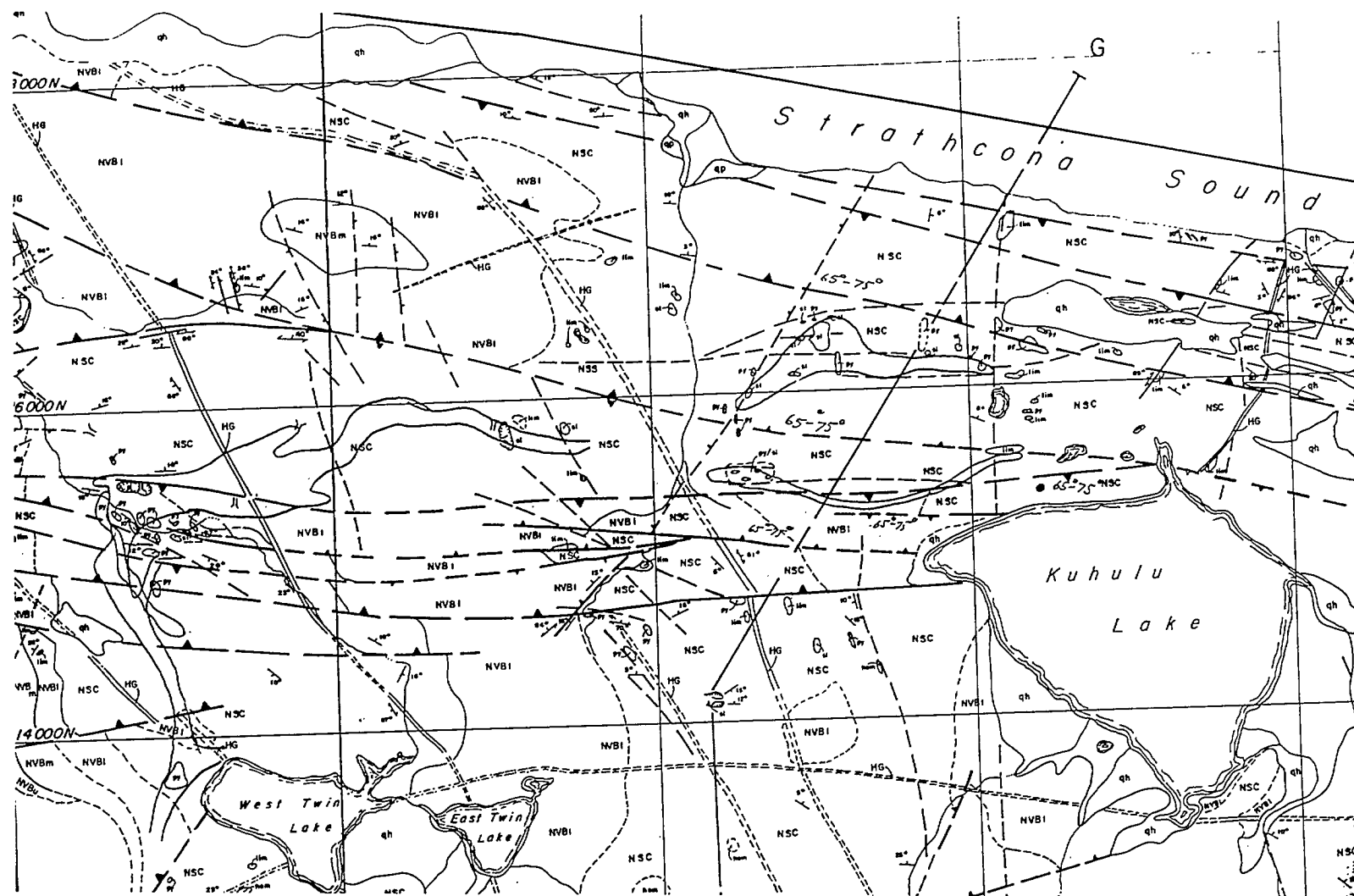


Fig. 3 - Geology Map, Nanisivik Ore Bodies

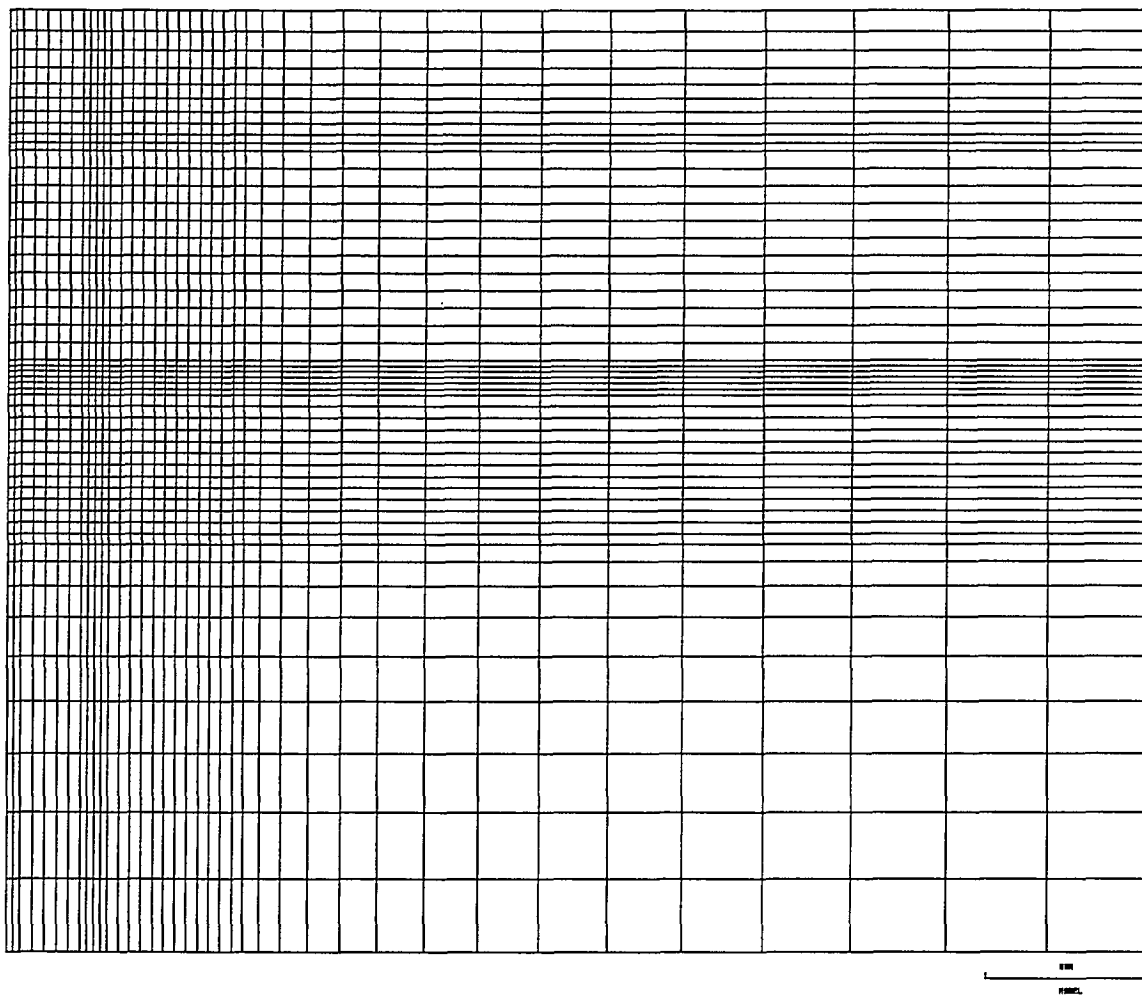


Fig. 4 - Finite Element Model 1, Variations of Crown Pillar Thickness

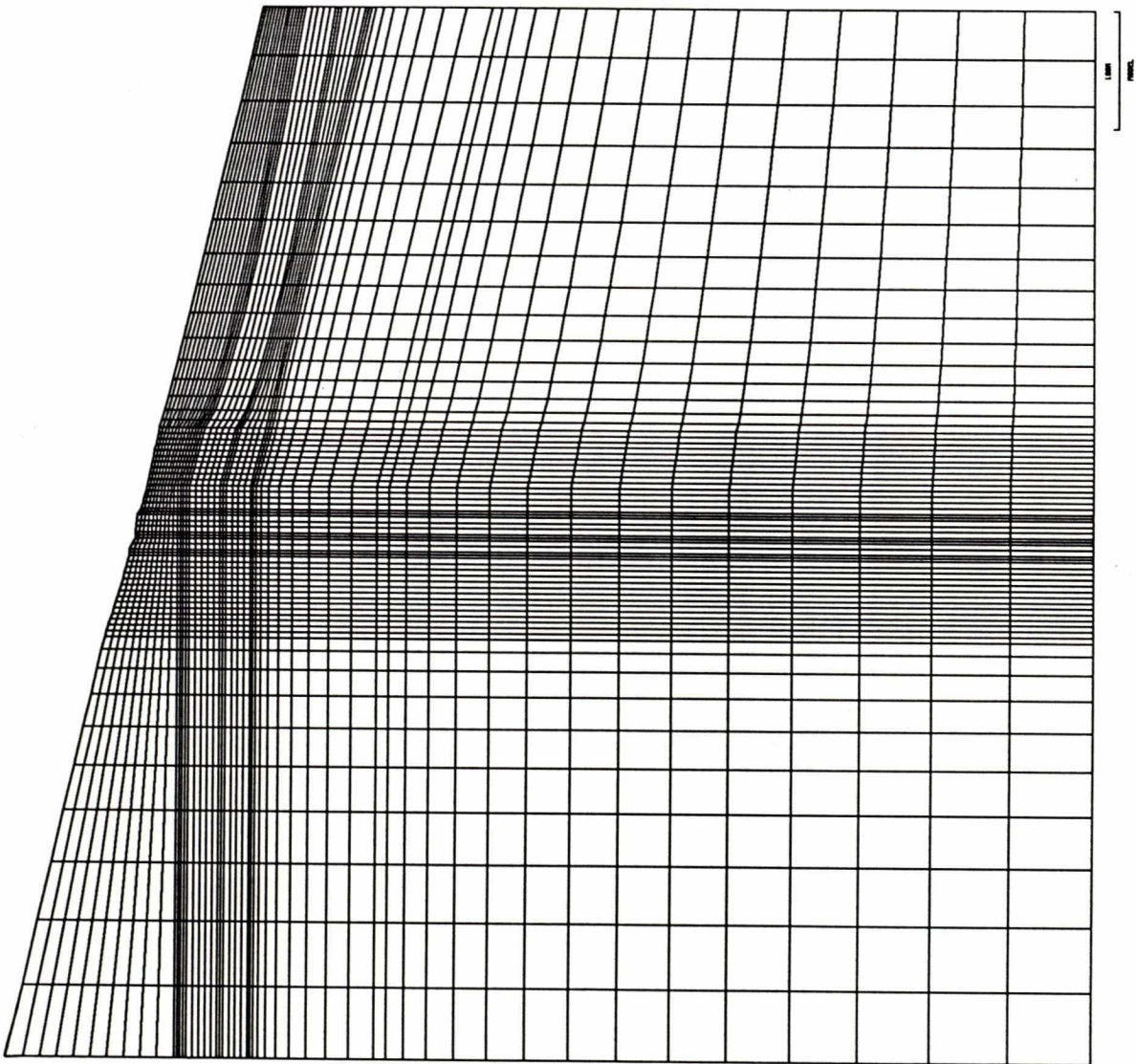


Fig. 5 - Finite Element Model 2, Cross-section 19250E

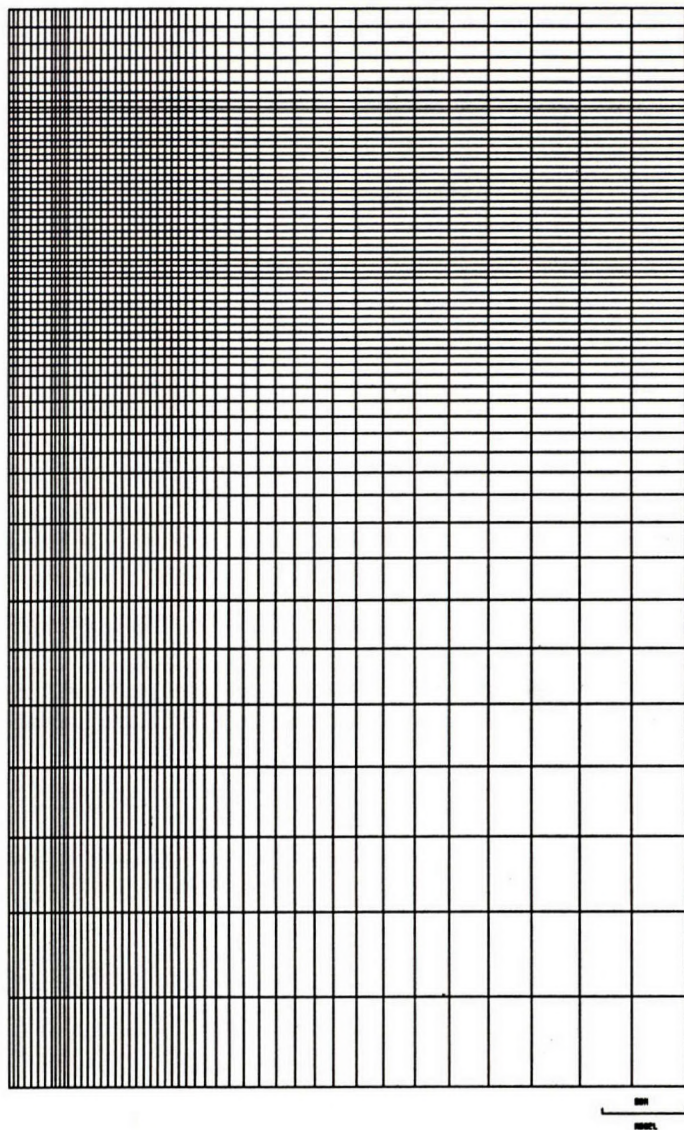


Fig. 6 - Finite Element Model 3, Cross-section 17800E

Legend

- ⊗ Relaxation Zone
- ⊙ High Tensile Stress Zone

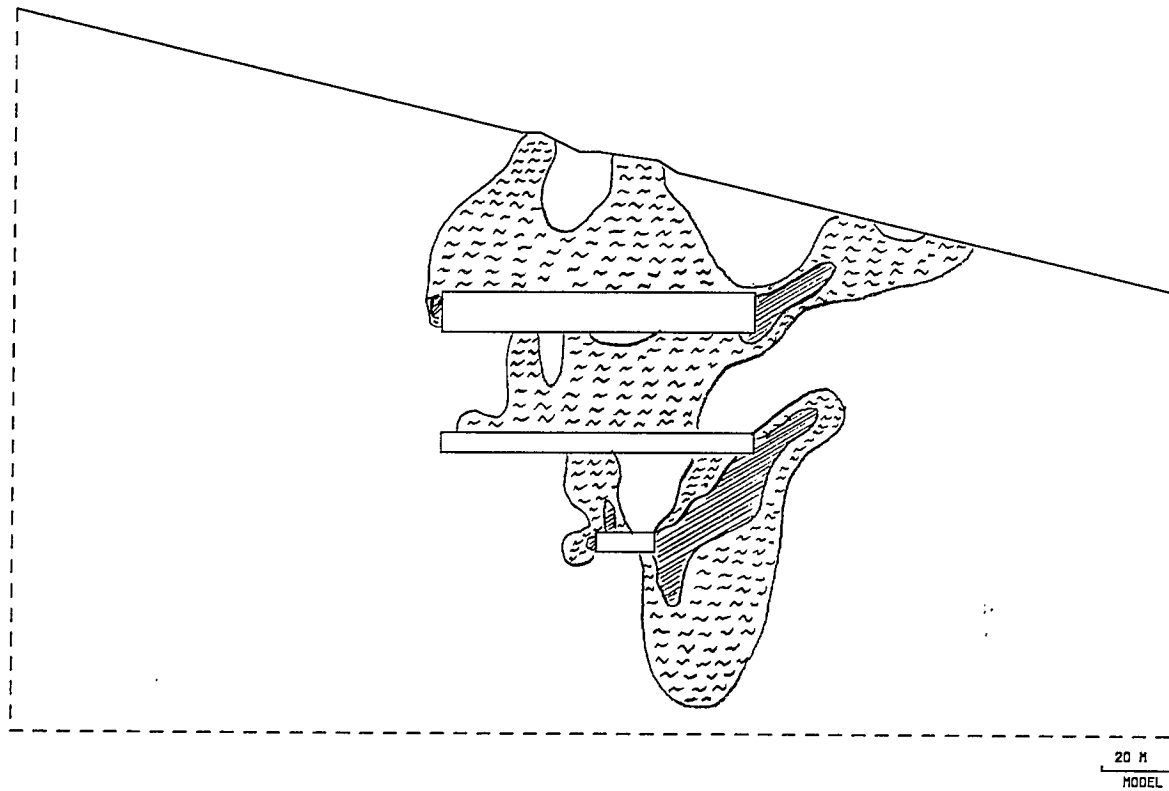


Fig. 7 - Relaxation Zones, Model 2, Section 19250E, Worst Condition

Legend

Cohesive Strength of Dolomite

— = 7 MPa

- - - = 6 MPa

... = 5 MPa

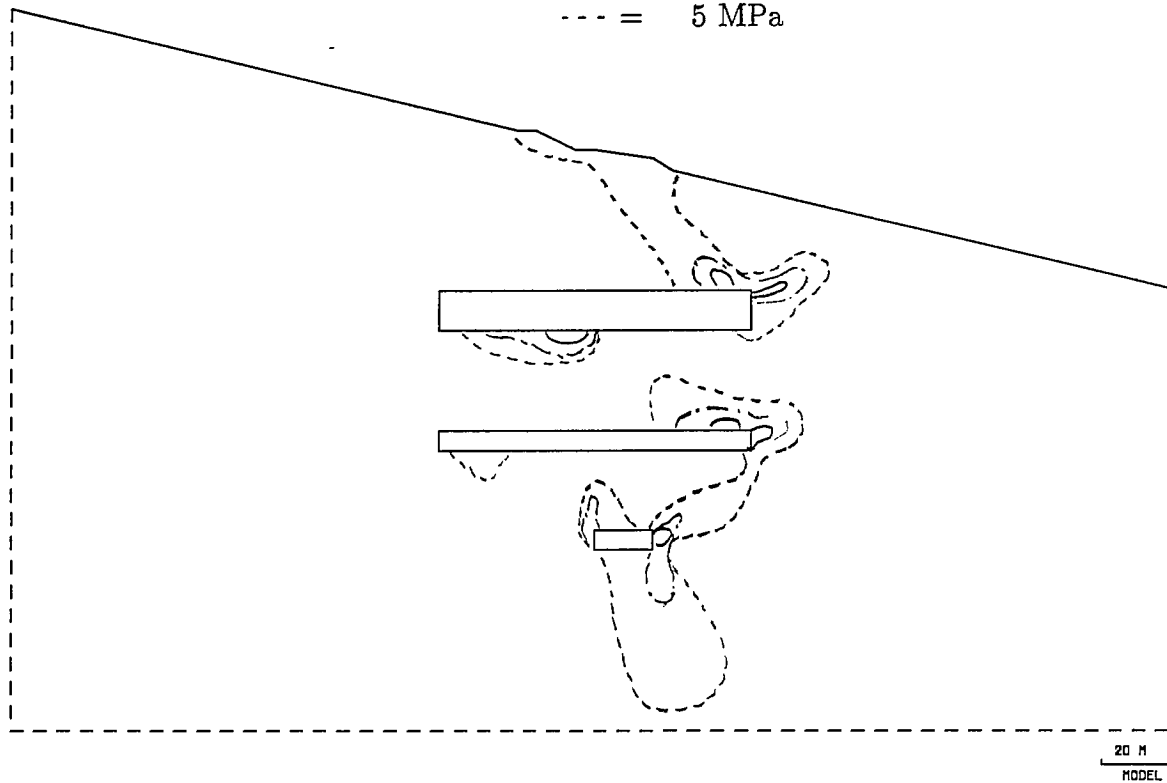
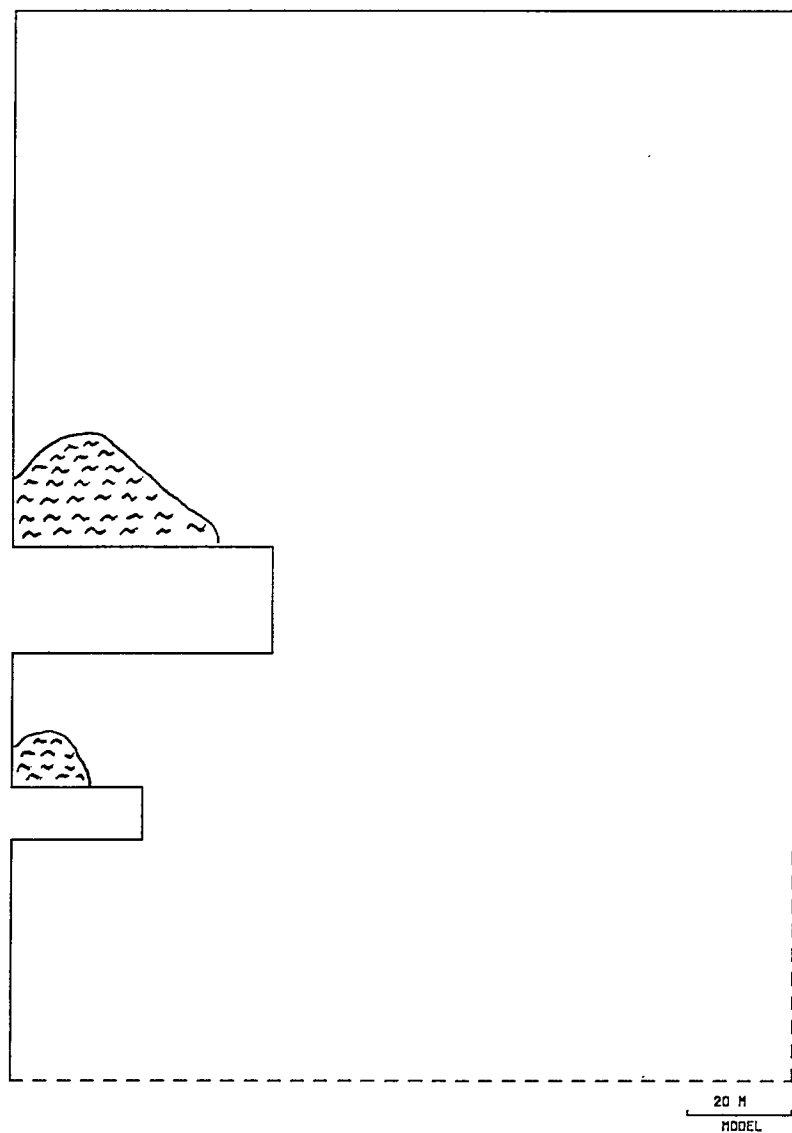


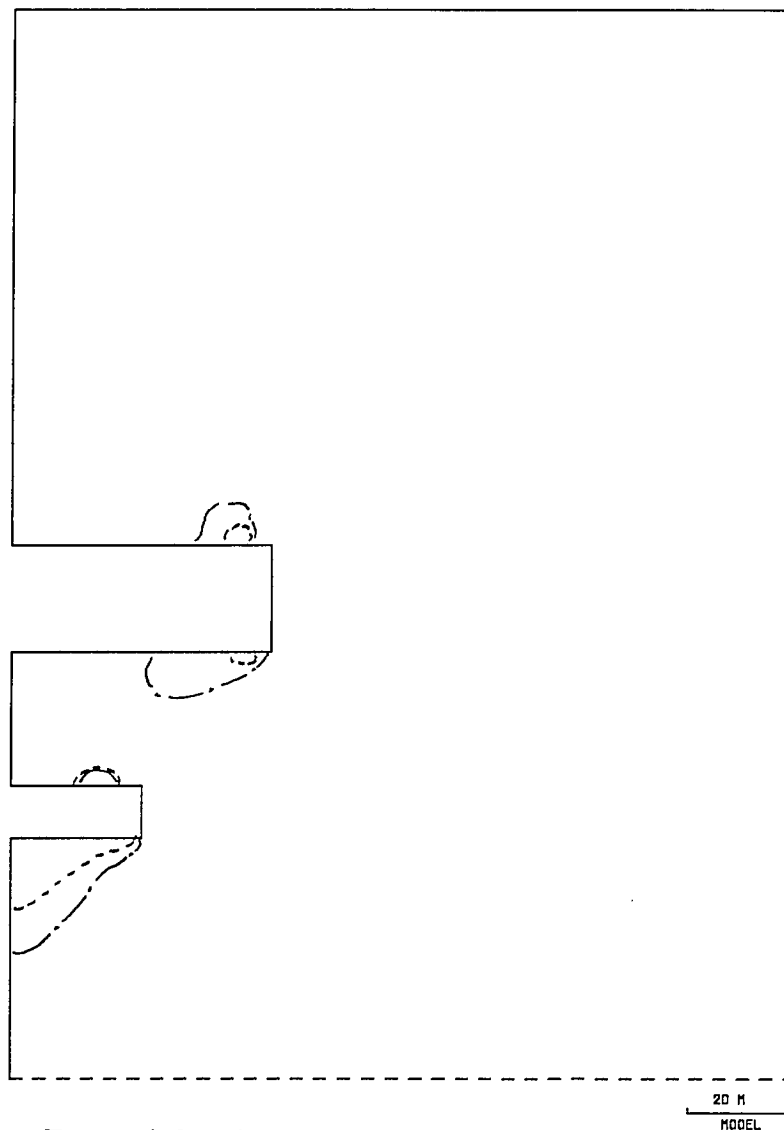
Fig. 8 - Potential Failure Zones, Model 2, Section 19250E, Worst Condition



Legend

⊗ Relaxation Zone

Fig. 9 - Relaxation Zones, Model 3, Section 17800E, Worst Condition



Legend

Cohesive Strength of Dolomite

— = 6 MPa

- - - = 4 MPa

- . - = 3 MPa

Fig. 10 - Potential Failure Zones, Model 3, Section 17800E, Worst Condition

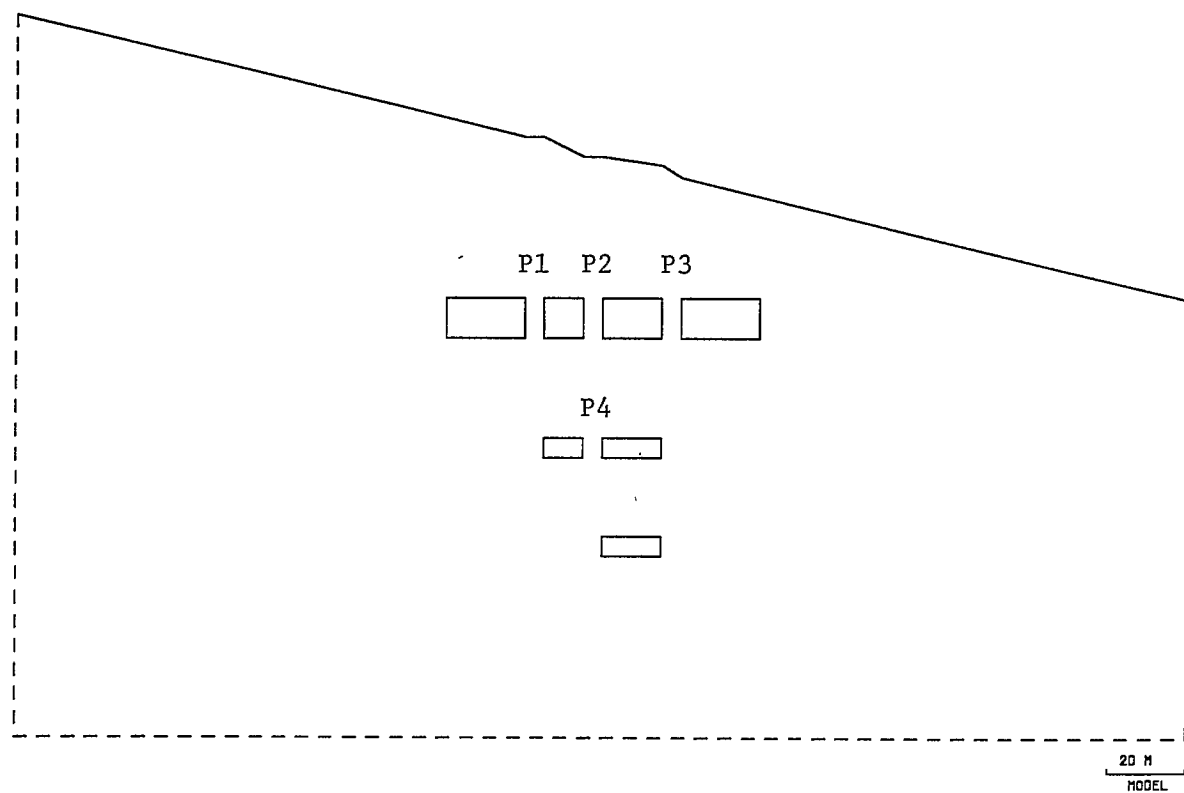


Fig. 11 - Sketch of Pillar Layout, Model 2, Section 19250E

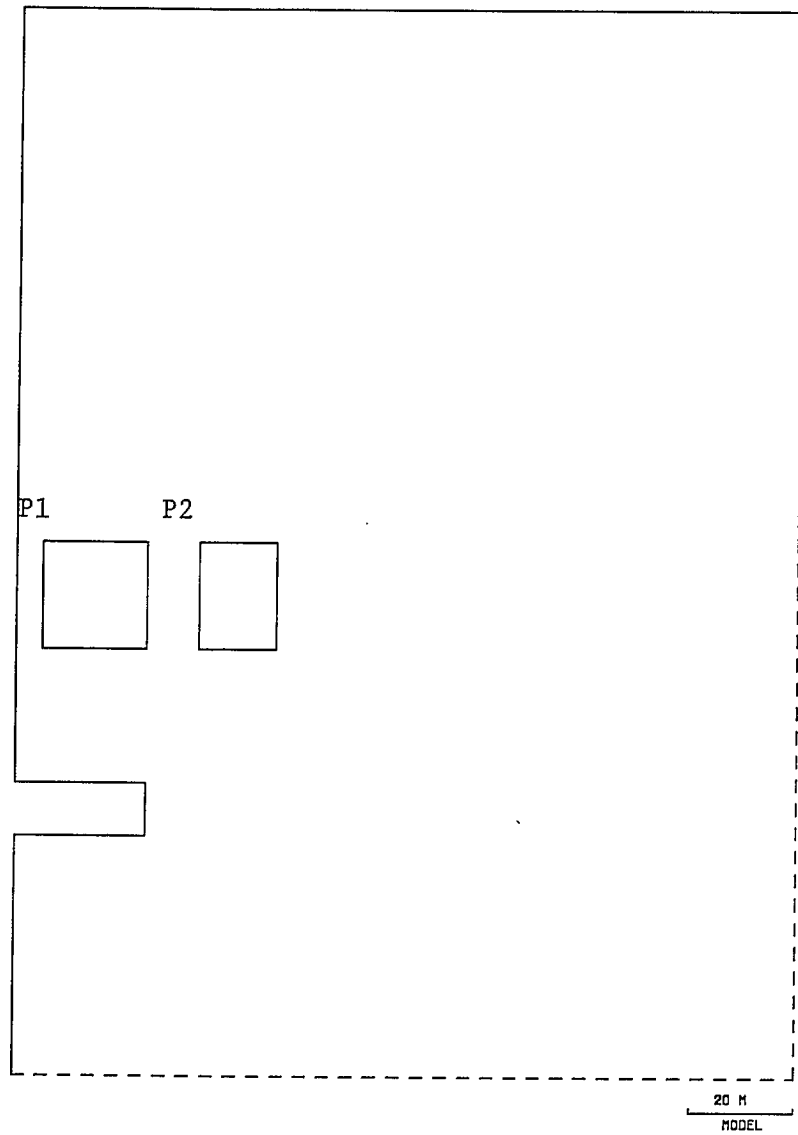


Fig. 12 - Sketch of Pillar Layout, Model 3, Section 17800E

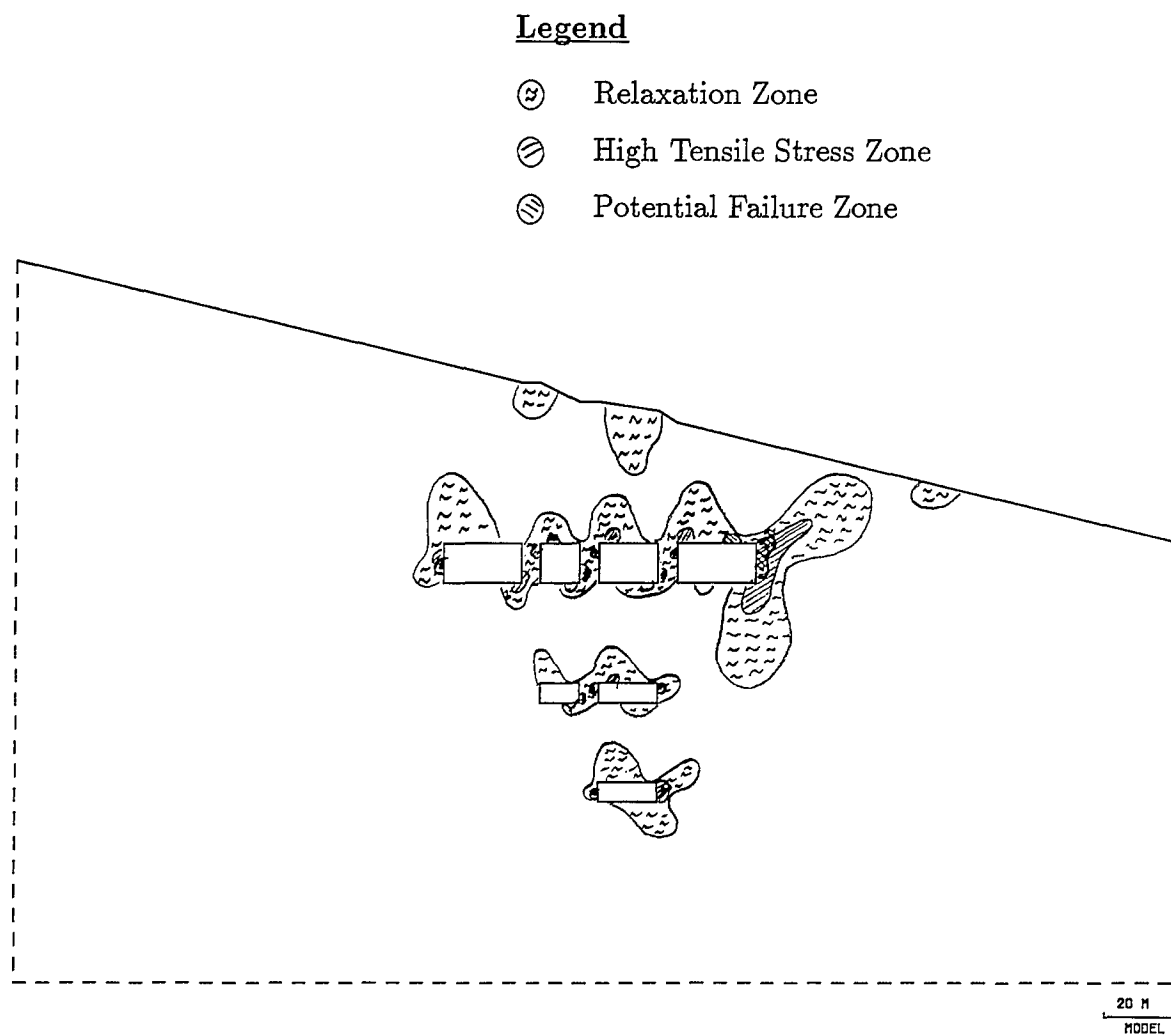


Fig. 13 - Relaxation Zones, Model 2, Section 19250E, Present Mining Stage

Legend

- ⊖ Relaxation Zone
- ⊗ High Tensile Stress Zone
- ⊕ Potential Failure Zone

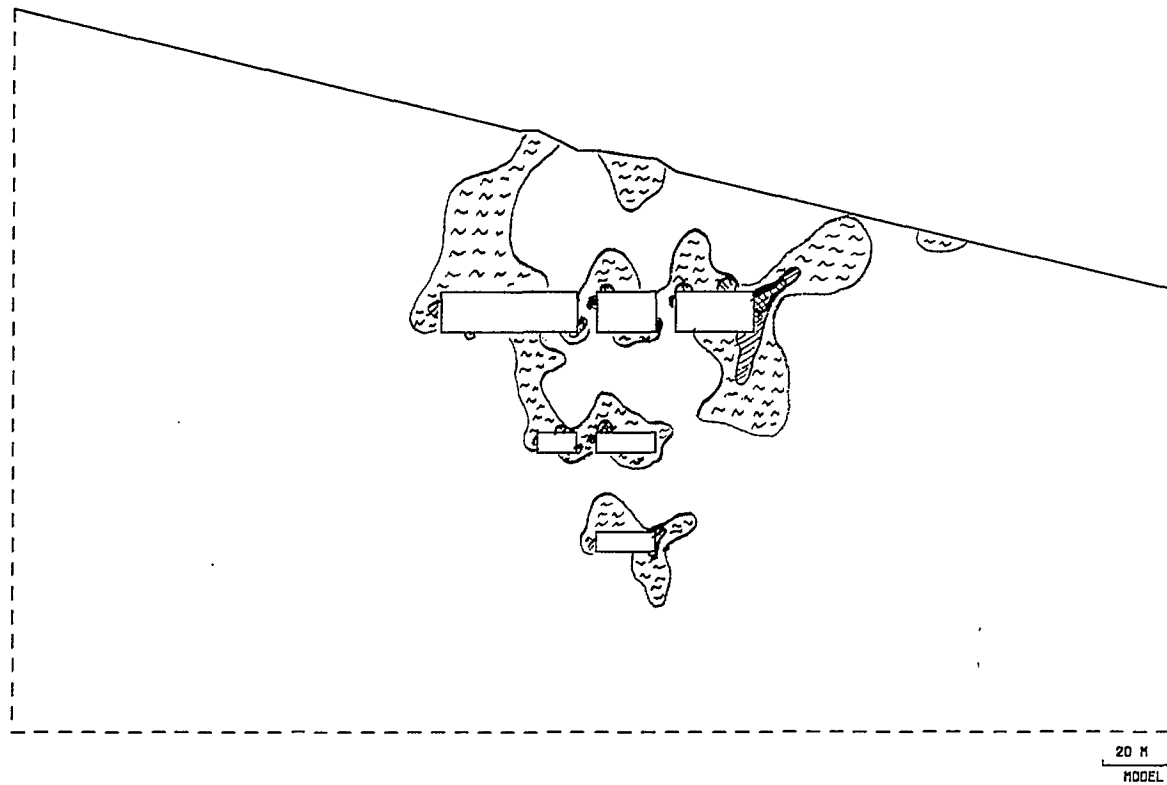


Fig. 14 - Relaxation Zones, Model 2, Section 19250E, P1 Mined

Legend

- ⊗ Relaxation Zone
- ⊘ High Tensile Stress Zone
- ⊙ Potential Failure Zone

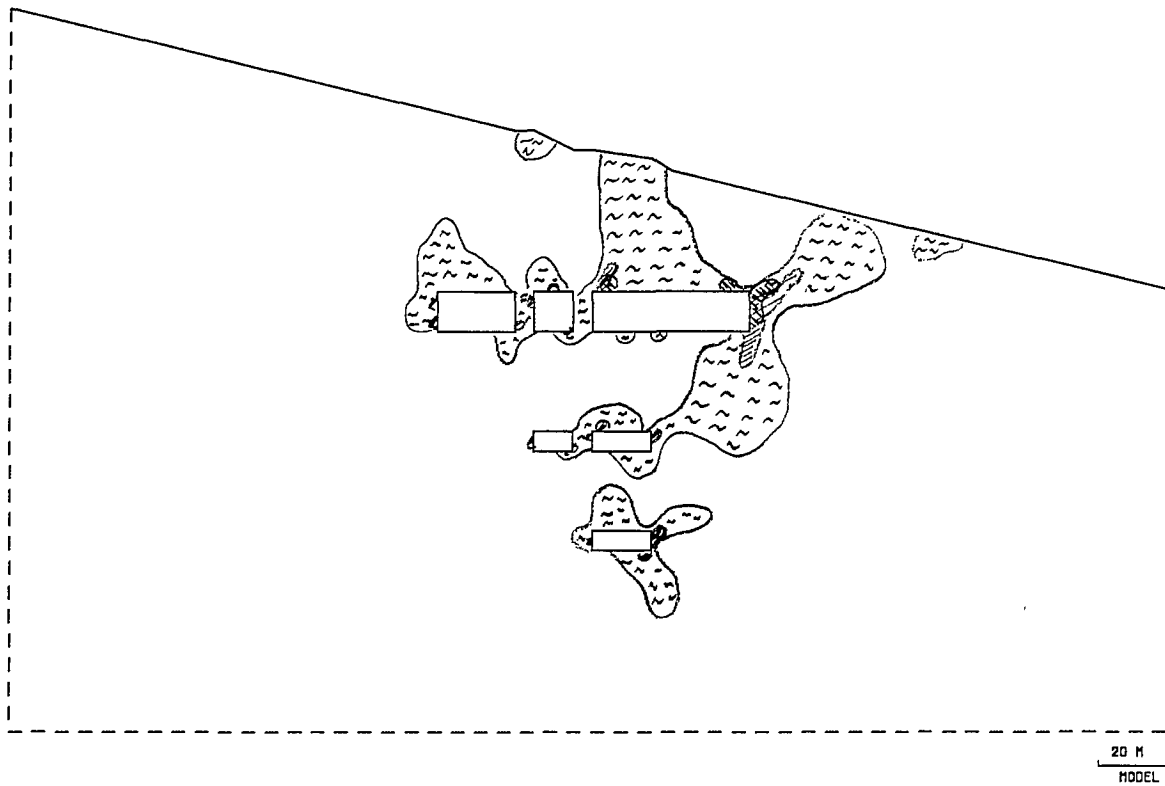


Fig. 15 - Relaxation Zones, Model 2, Section 19250E, P3 Mined

Legend

- ⊗ Relaxation Zone
- ⊙ High Tensile Stress Zone
- ⊖ Potential Failure Zone

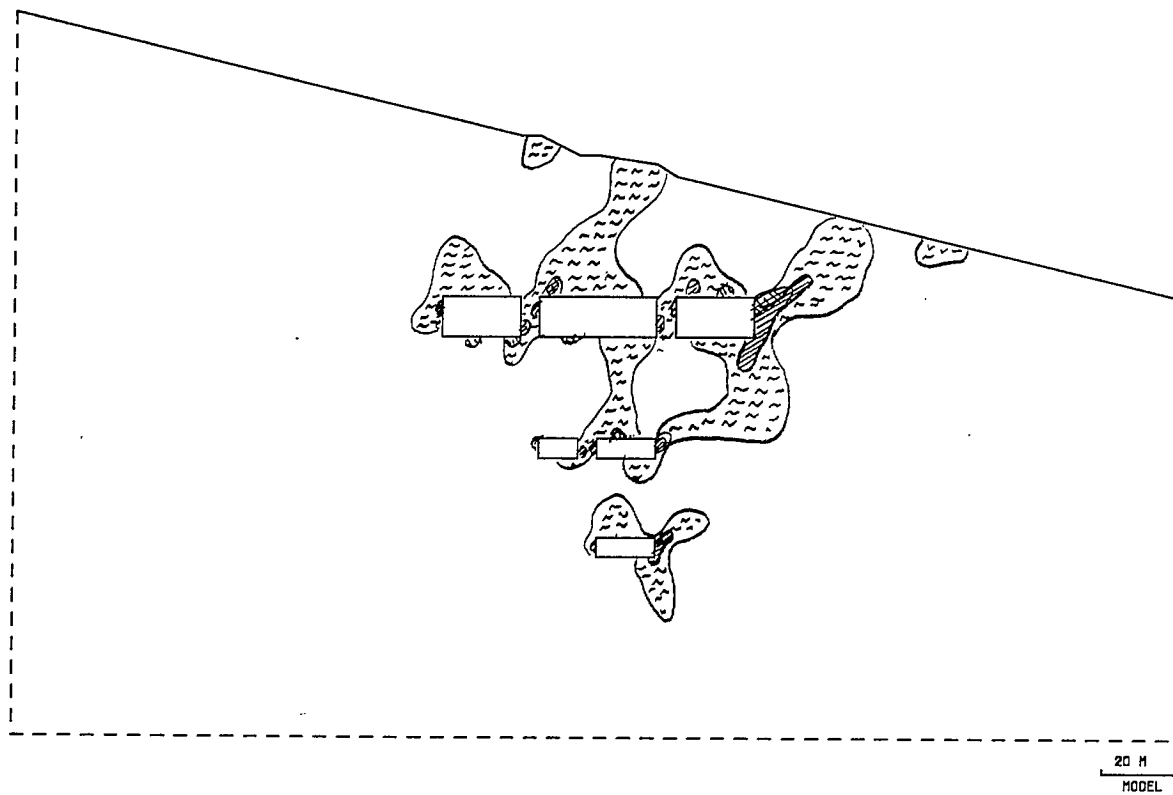


Fig. 16 - Relaxation Zones, Model 2, Section 19250E, P2 Mined

Legend

- ⊙ Relaxation Zone
- ⊙ High Tensile Stress Zone
- ⊙ Potential Failure Zone

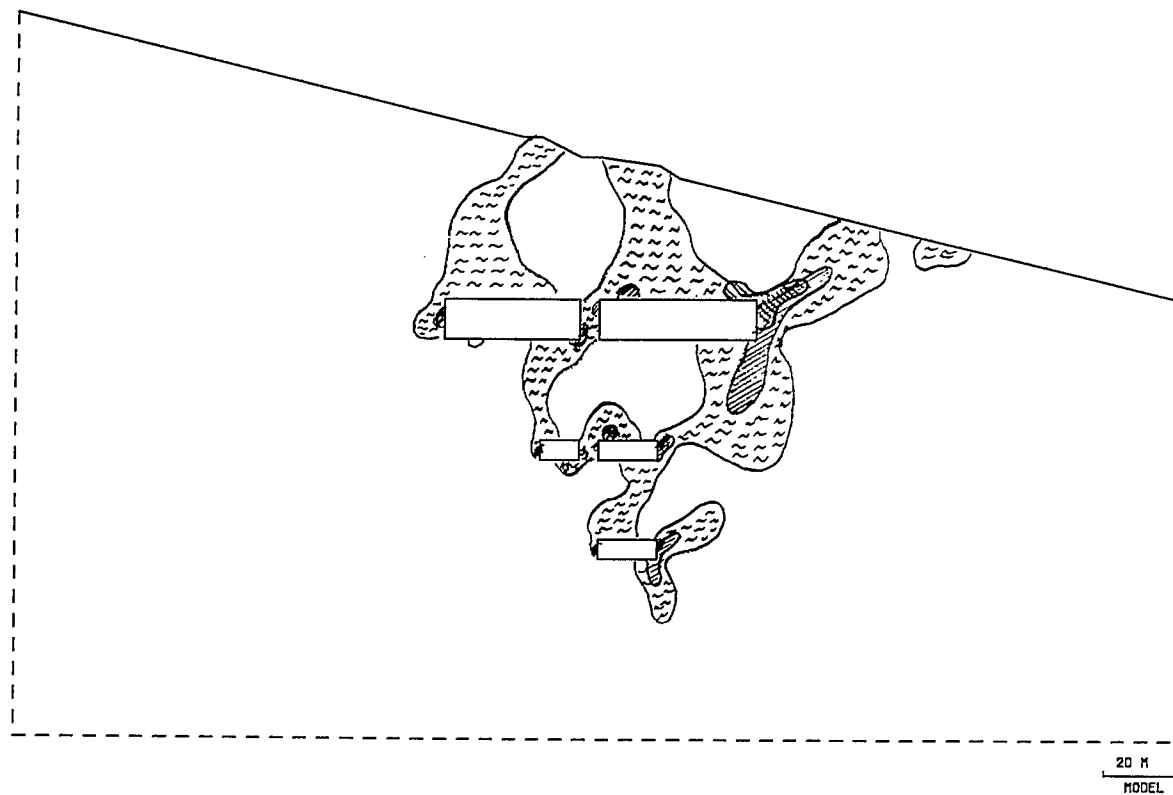


Fig. 17 - Relaxation Zones, Model 2, Section 19250E, P1, P3 Mined

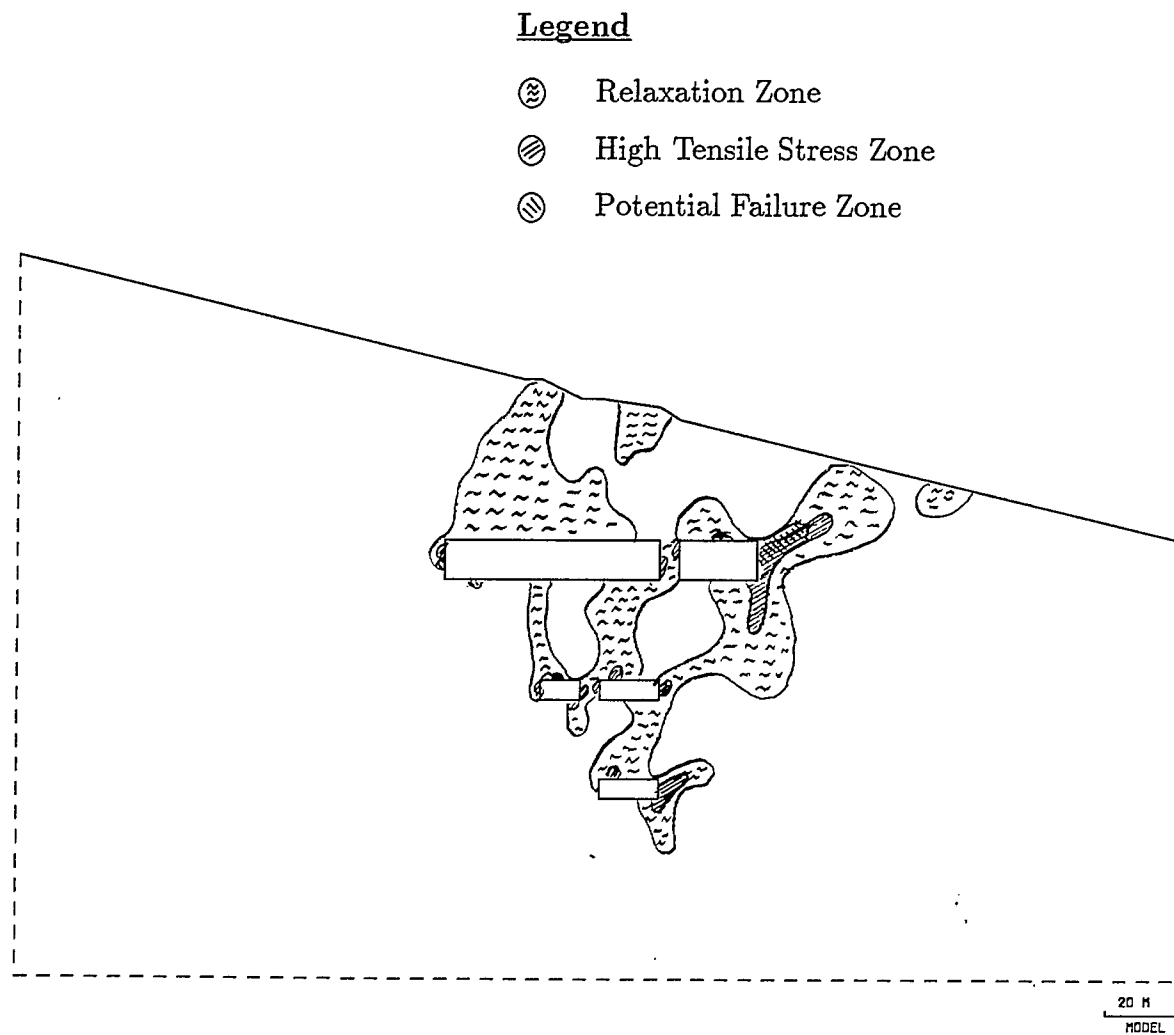


Fig. 18 - Relaxation Zones, Model 2, Section 19250E, P1, P2 Mined

Legend

- ⊗ Relaxation Zone
- ⊗ High Tensile Stress Zone
- ⊗ Potential Failure Zone

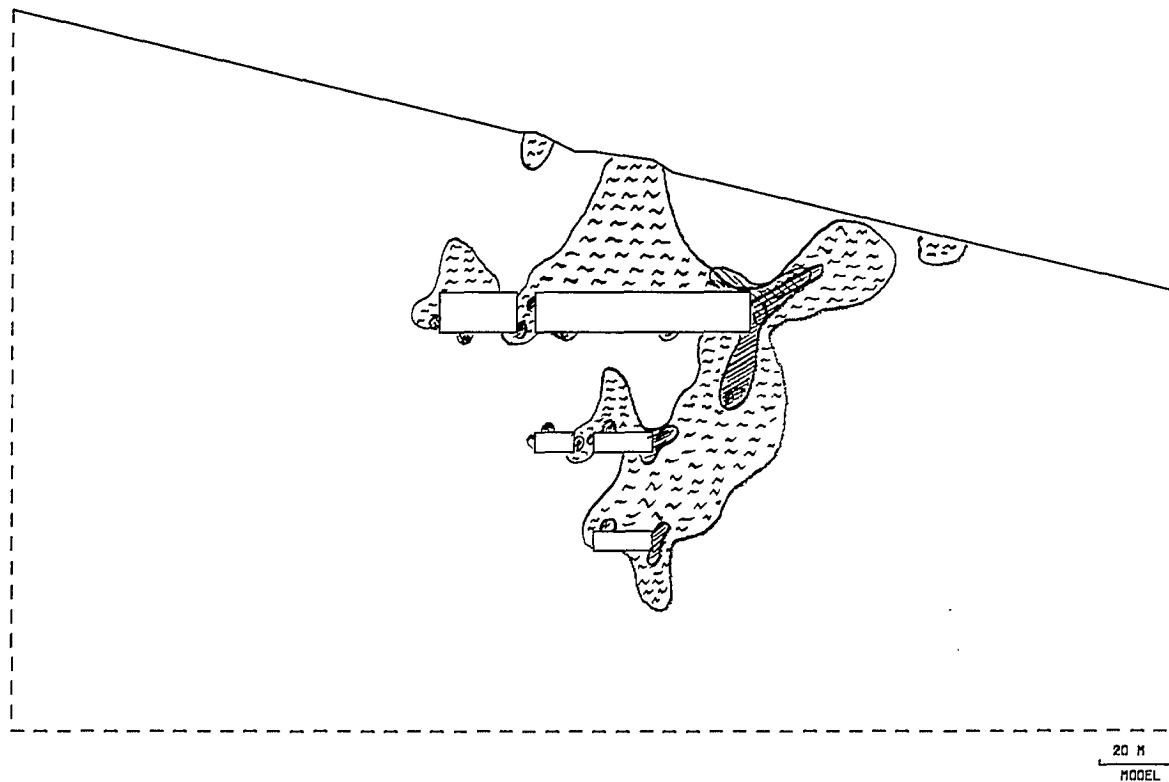


Fig. 19 - Relaxation Zones, Model 2, Section 19250E, P2, P3 Mined

Legend

- ⊗ Relaxation Zone
- ⊗ High Tensile Stress Zone
- ⊗ Potential Failure Zone

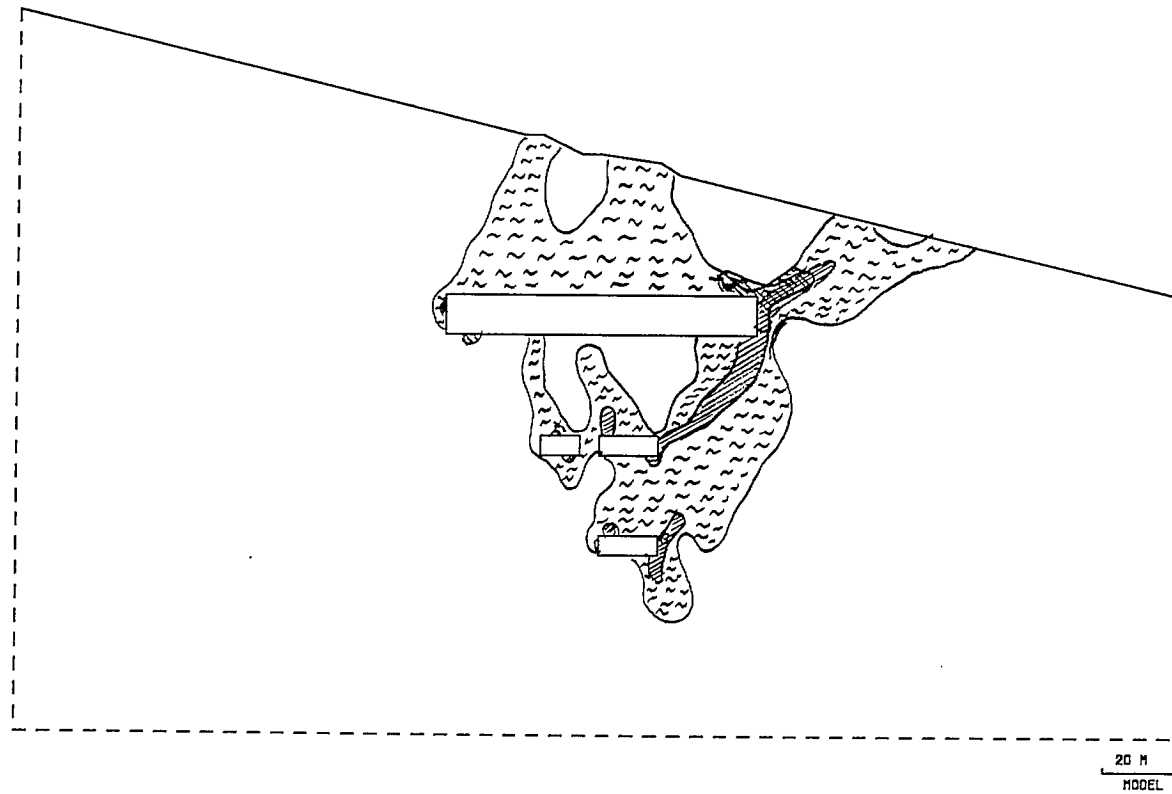


Fig. 20 - Relaxation Zones, Model 2, Section 19250E, P1, P2, P3 Mined

Legend

- ⊗ Relaxation Zone
- ⊙ High Tensile Stress Zone
- ⊘ Potential Failure Zone

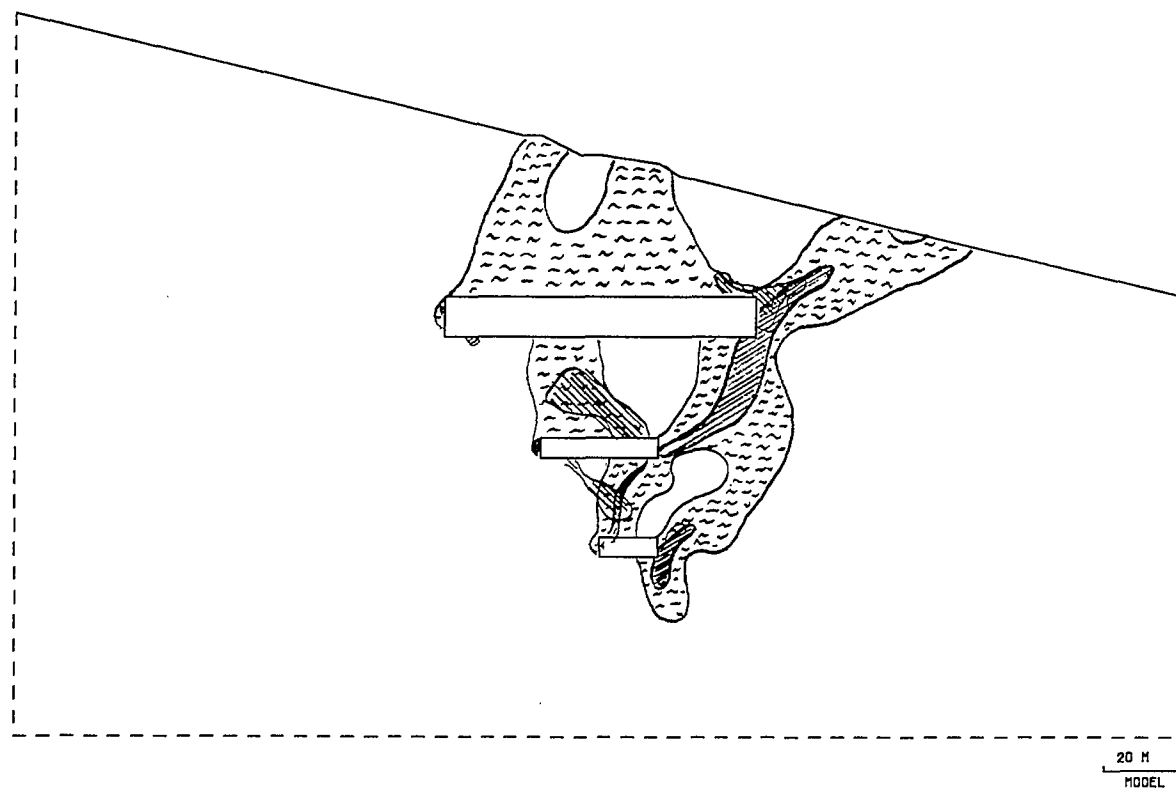


Fig. 21 - Relaxation Zones, Model 2, Section 19250E, P1, P2, P3, P4 Mined

Legend

- ⊗ Relaxation Zone
- ⊗ High Tensile Stress Zone
- ⊗ Potential Failure Zone

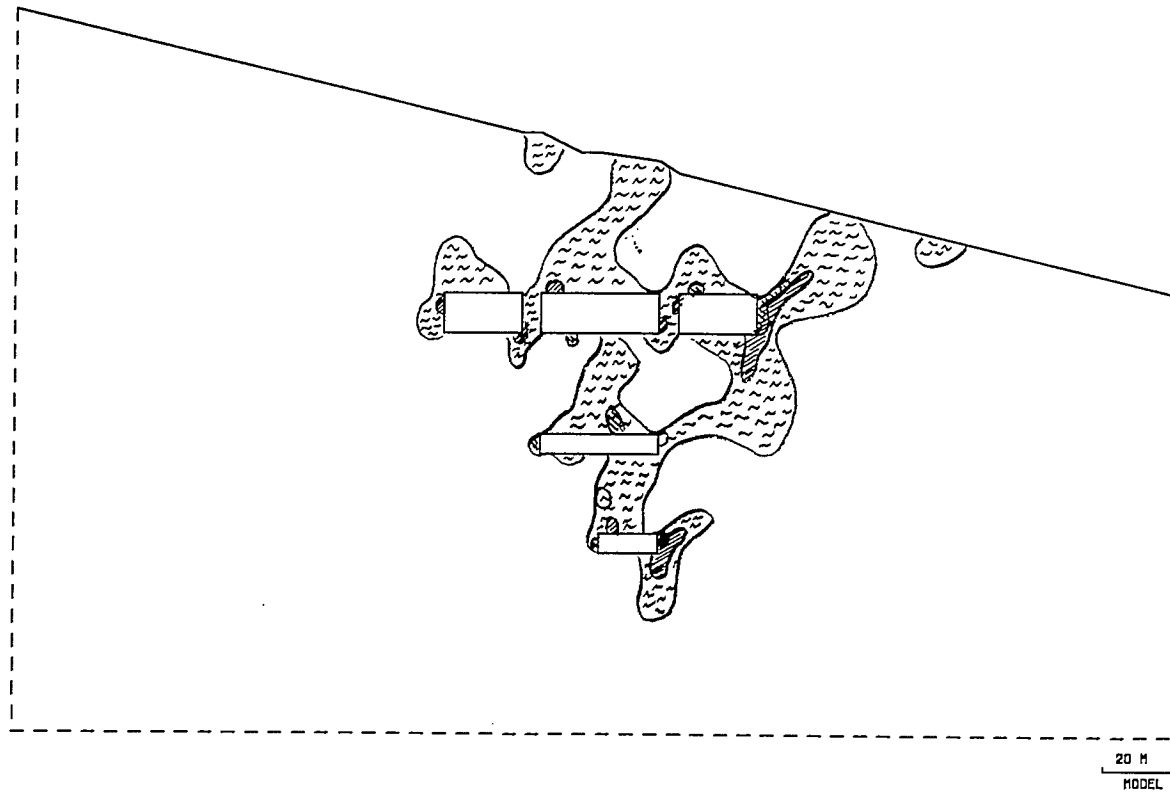


Fig. 22 - Relaxation Zones, Model 2, Section 19250E, P2, P4 Mined

Legend

- ⊗ Relaxation Zone
- ⊙ High Tensile Stress Zone
- ⊖ Potential Failure Zone

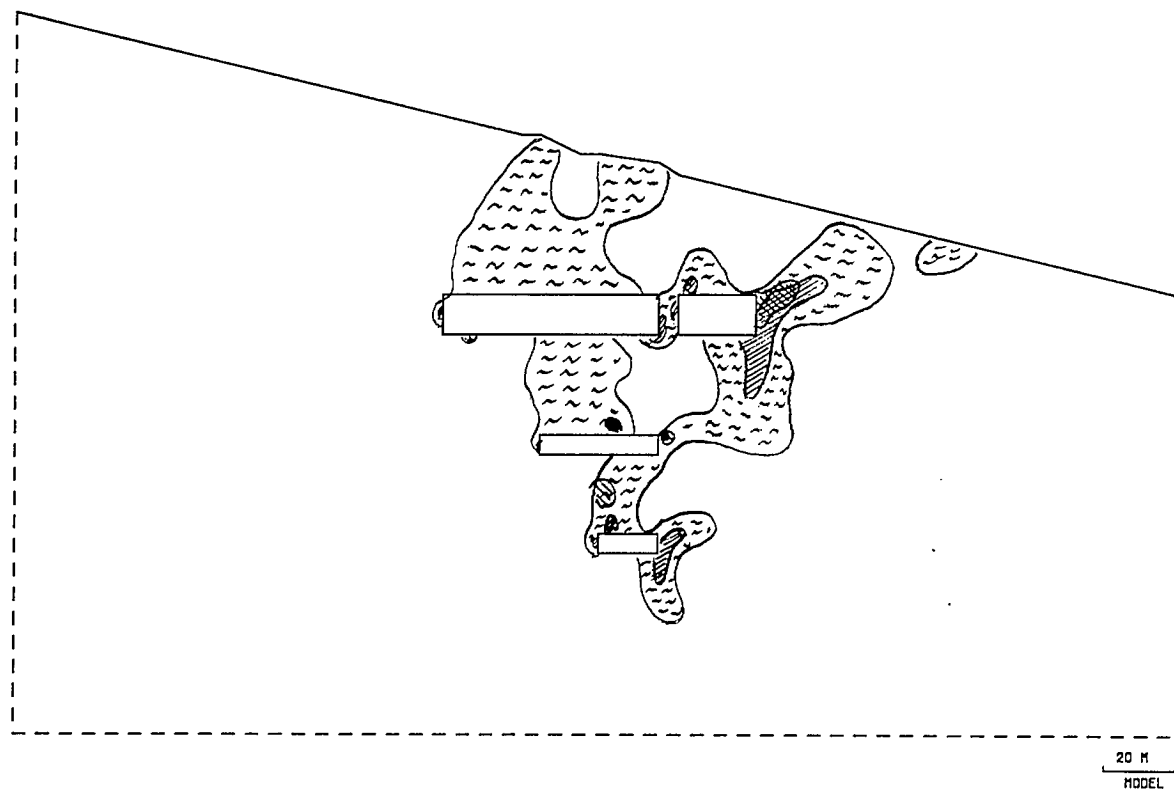


Fig. 23 - Relaxation Zones, Model 2, Section 19250E, P1, P2, P4 Mined

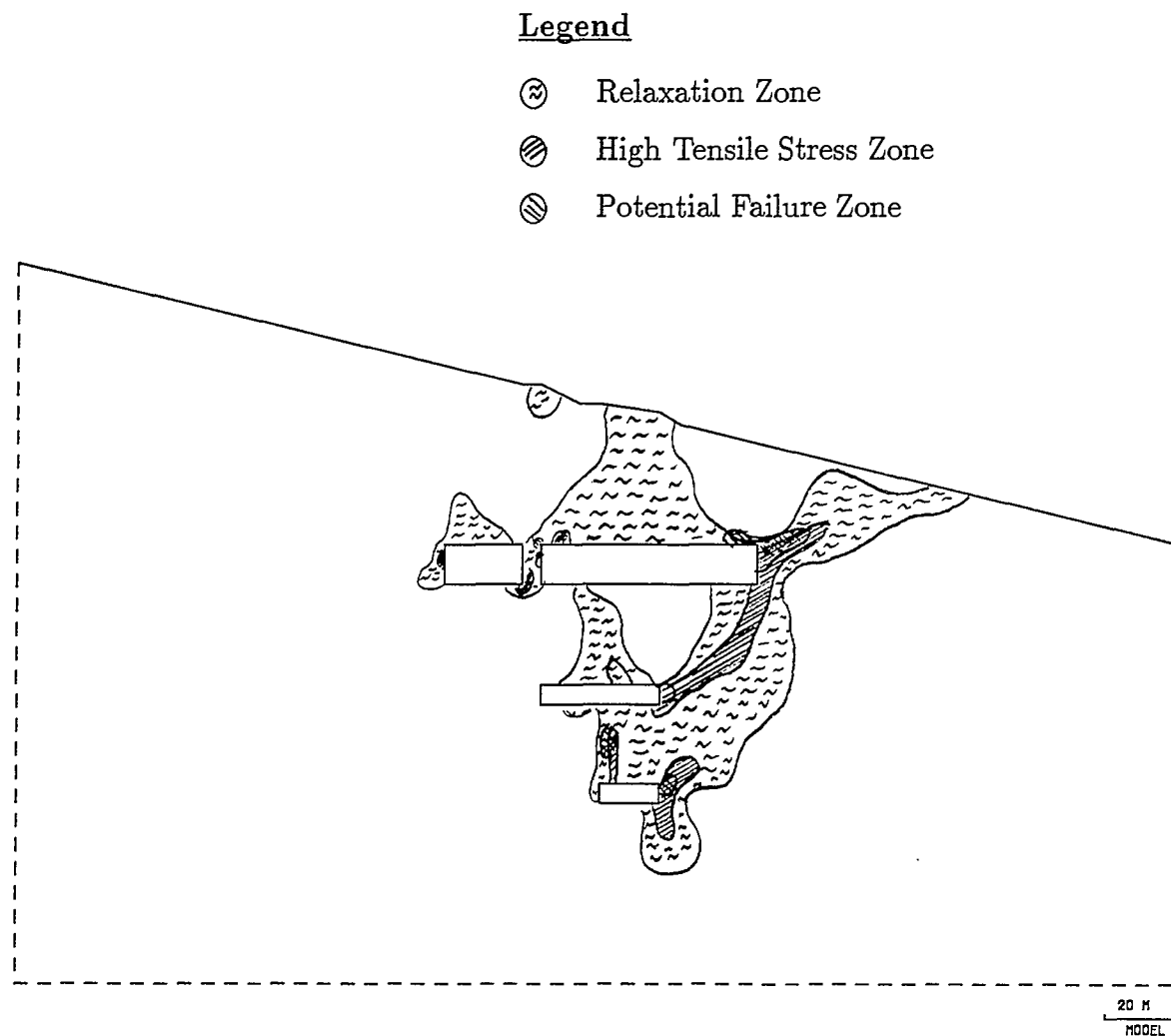


Fig. 24 - Relaxation Zones, Model 2, Section 19250E, P2, P3, P4 Mined

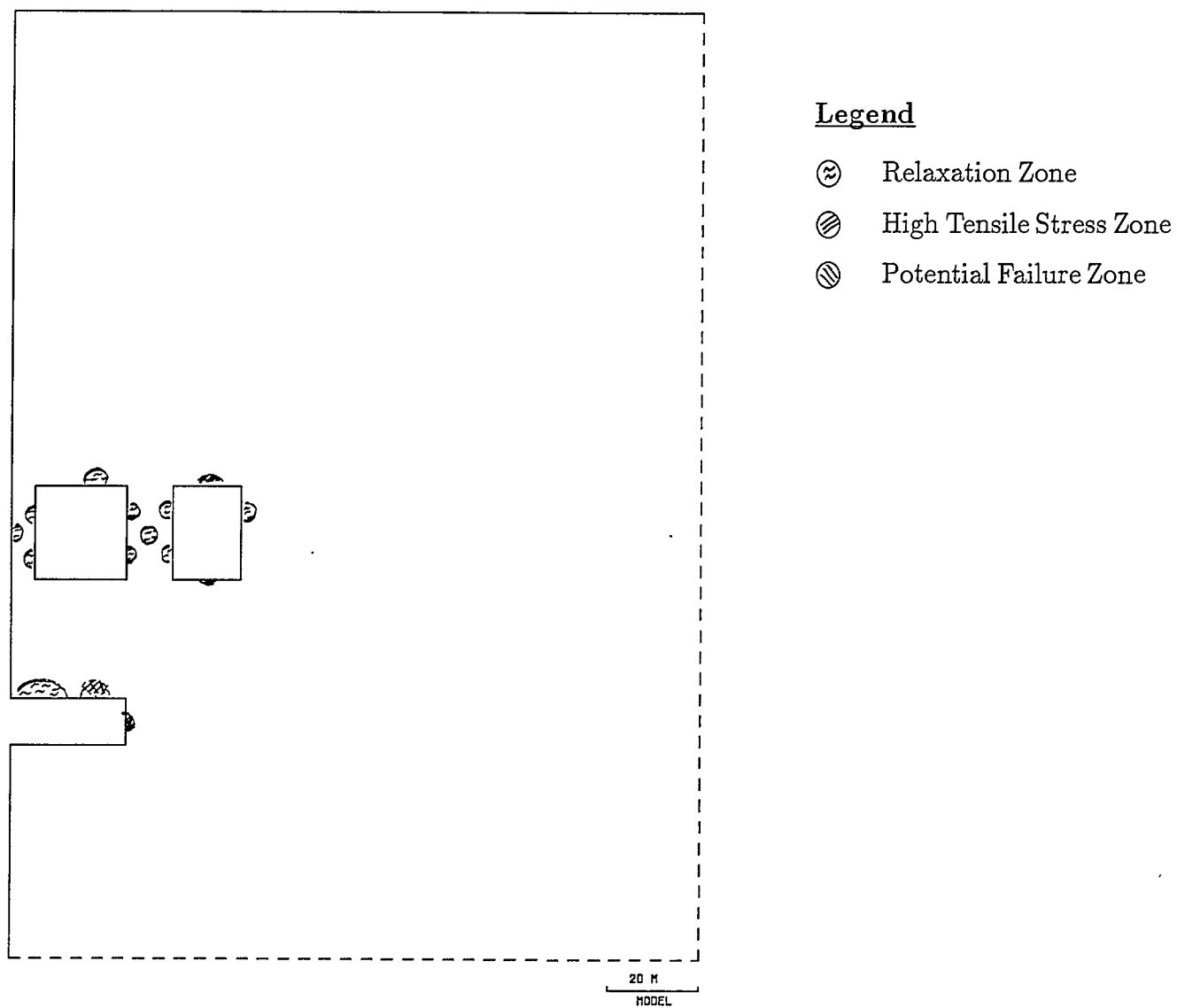


Fig. 25 - Relaxation Zones, Model 3, Section 17800E, Present Mining Stage

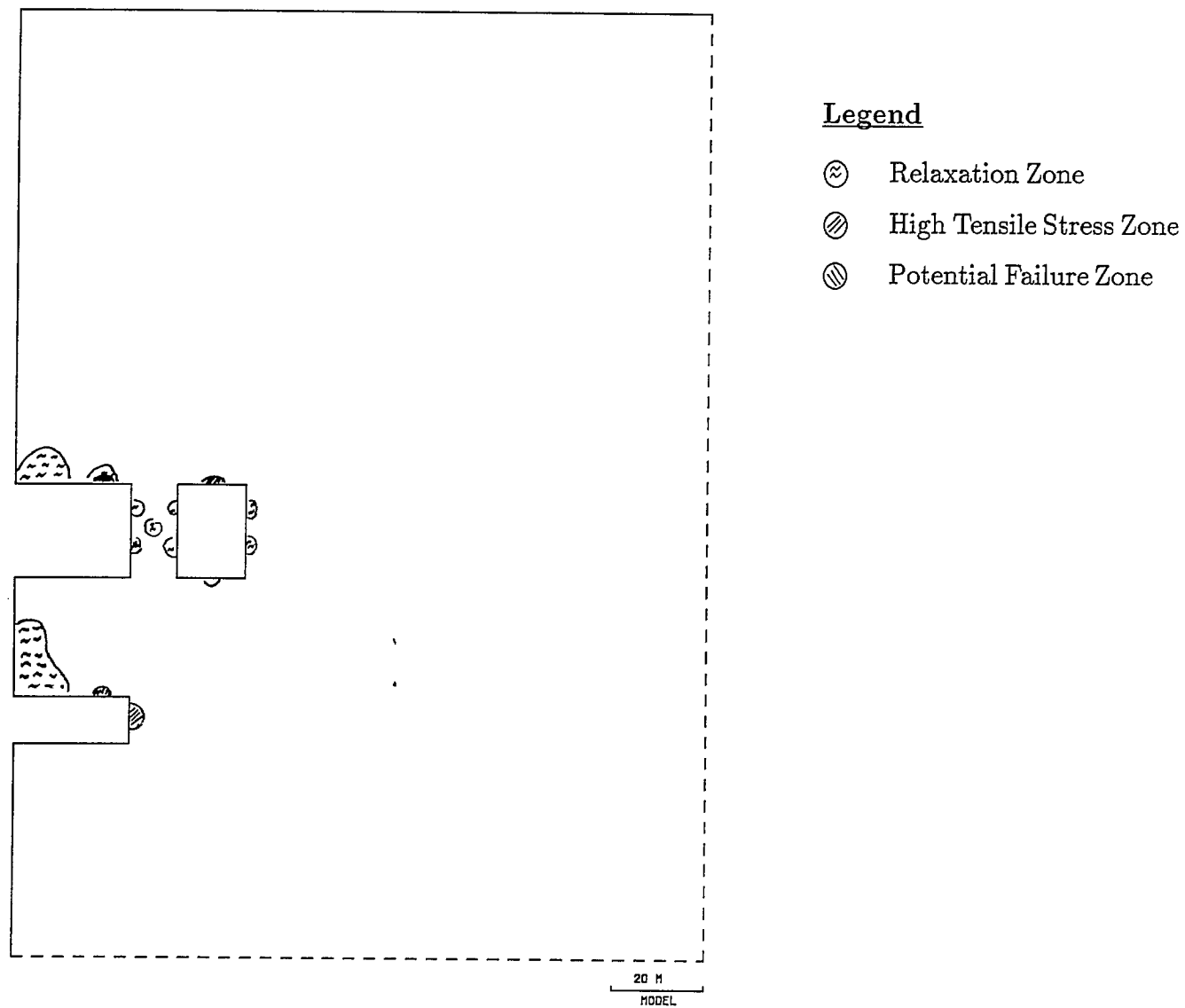


Fig. 26 - Relaxation Zones, Model 3, Section 17800E, P1 Mined

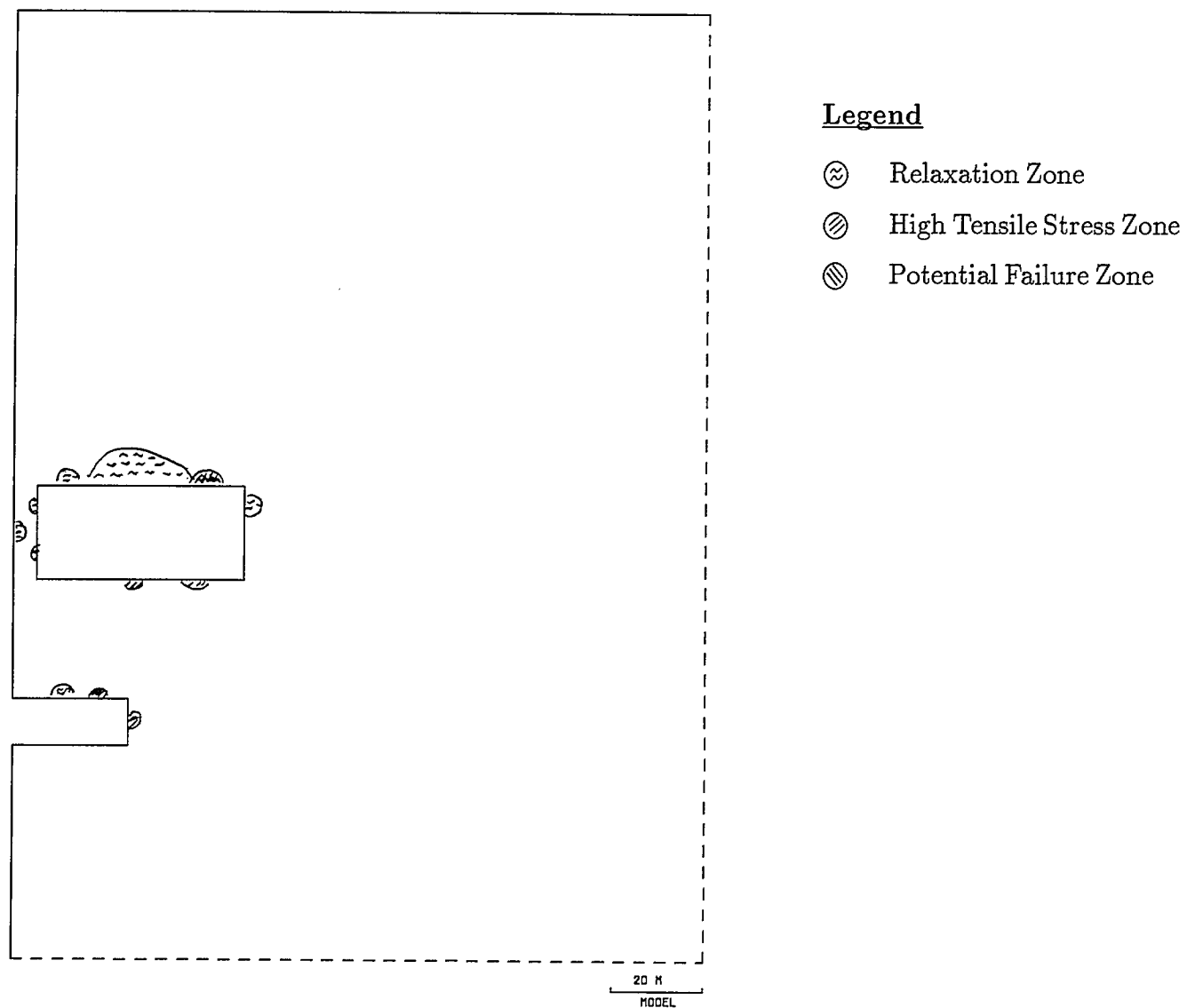


Fig. 27 - Relaxation Zones, Model 3, Section 17800E, P2 Mined

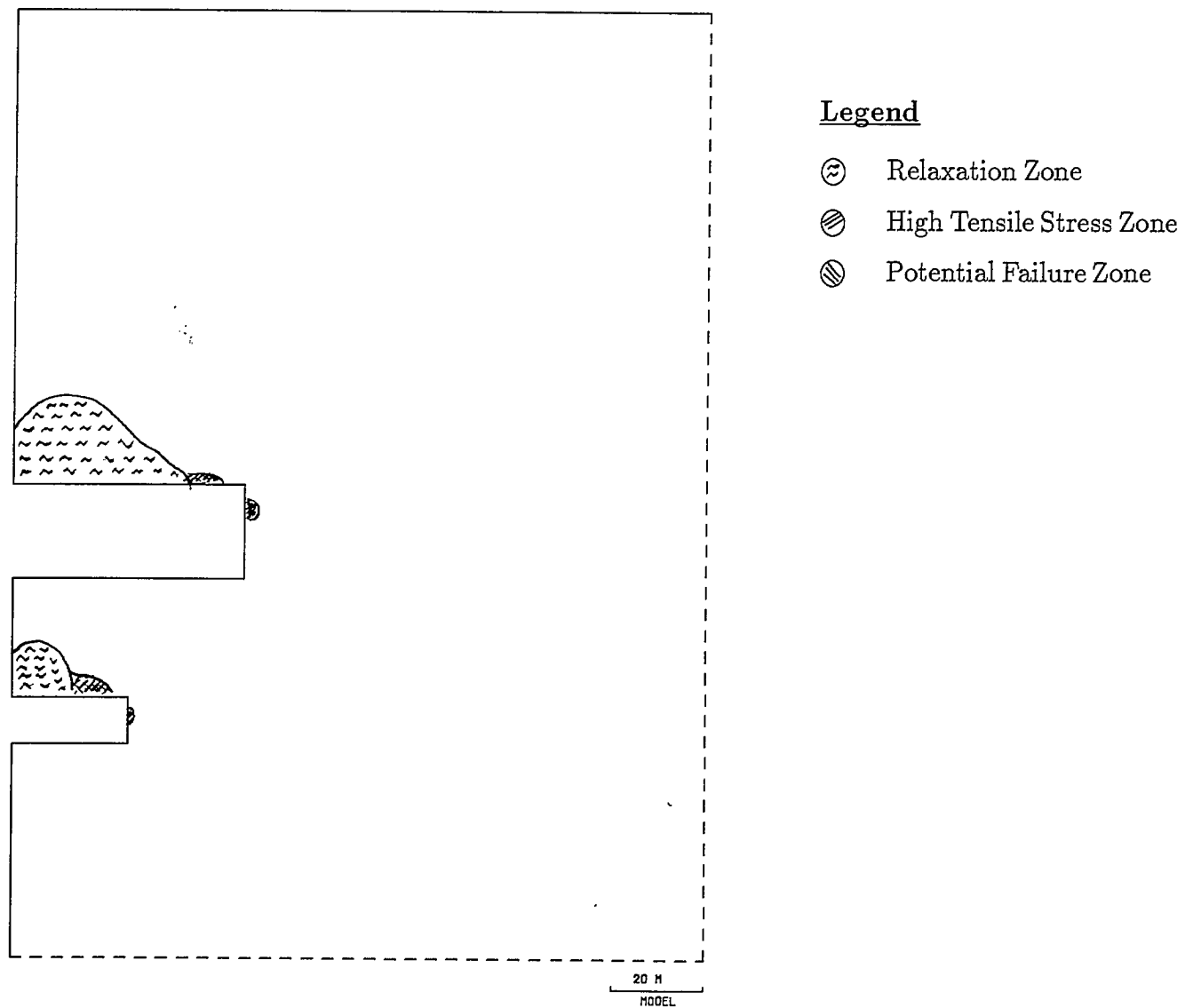


Fig. 28 - Relaxation Zones, Model 3, Section 17800E, P1, P2 Mined

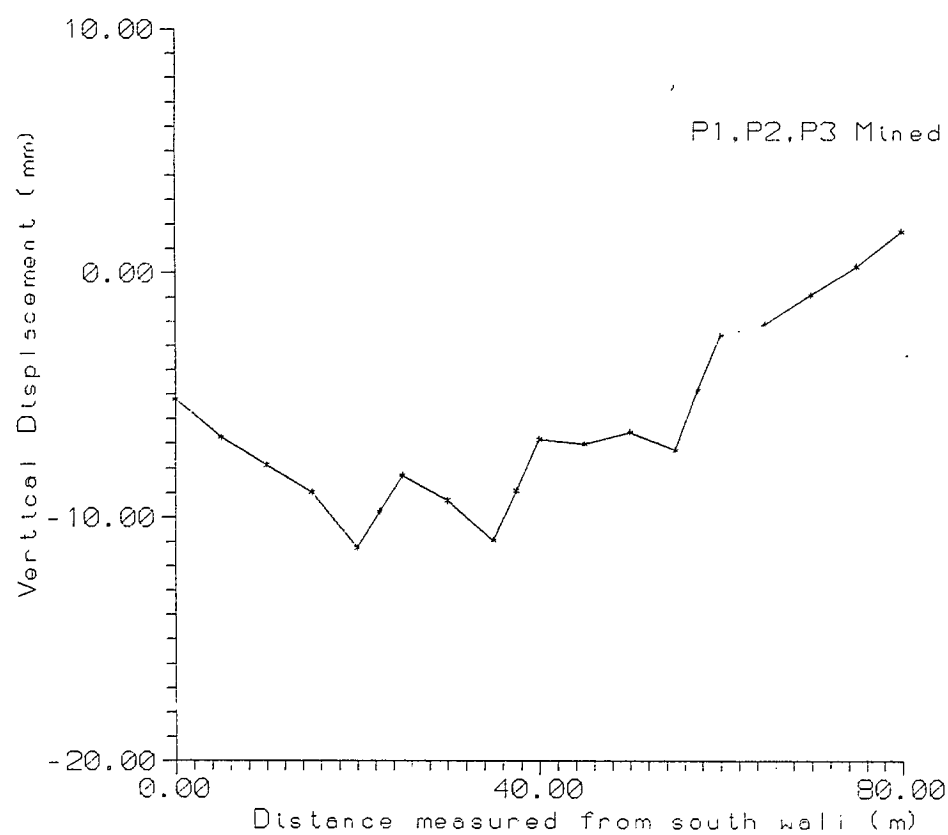


Fig. 29 - Excavation Displacements At Stope Roof, Model 2, Section 19250E

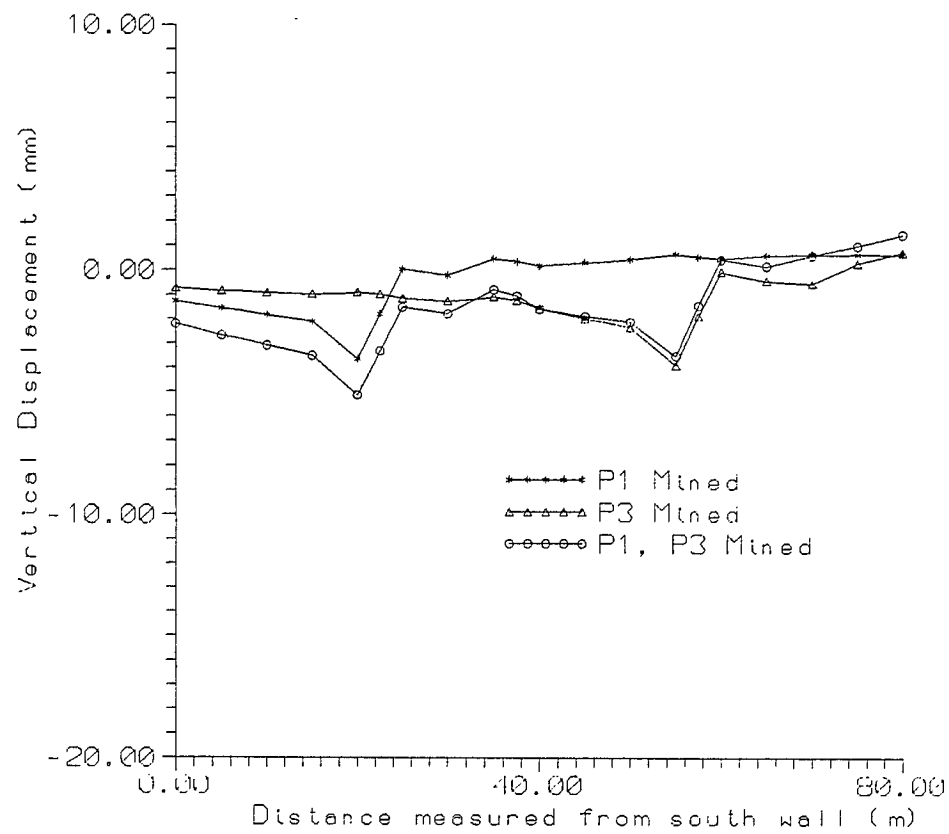


Fig. 30 - Excavation Displacements At Stope Roof, Model 2, Section 19250E

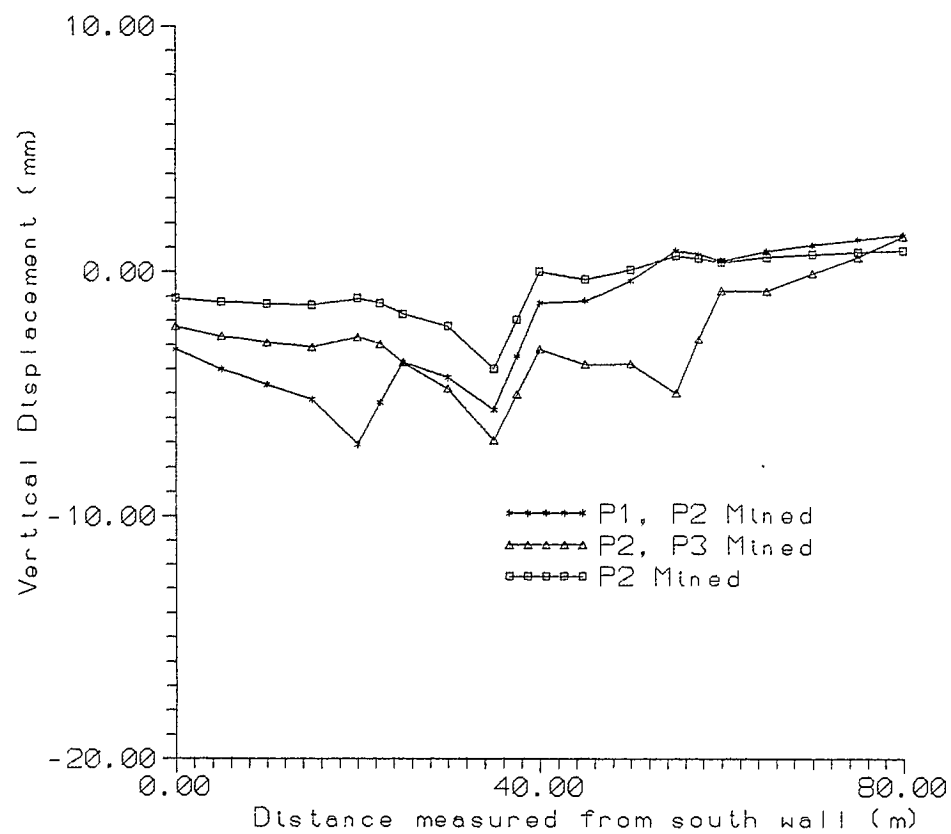


Fig. 31 - Excavation Displacements At Stope Roof, Model 2, Section 19250E

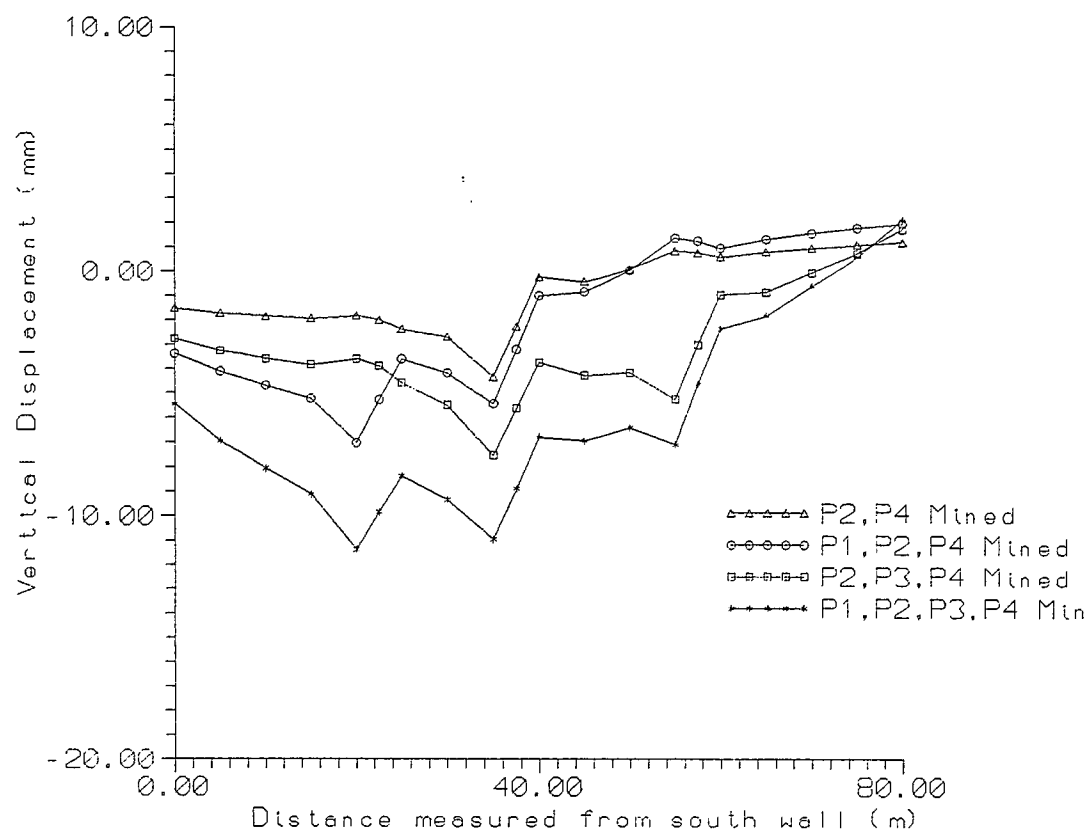


Fig. 32 - Excavation Displacements At Stope Roof, Model 2, Section 19250E

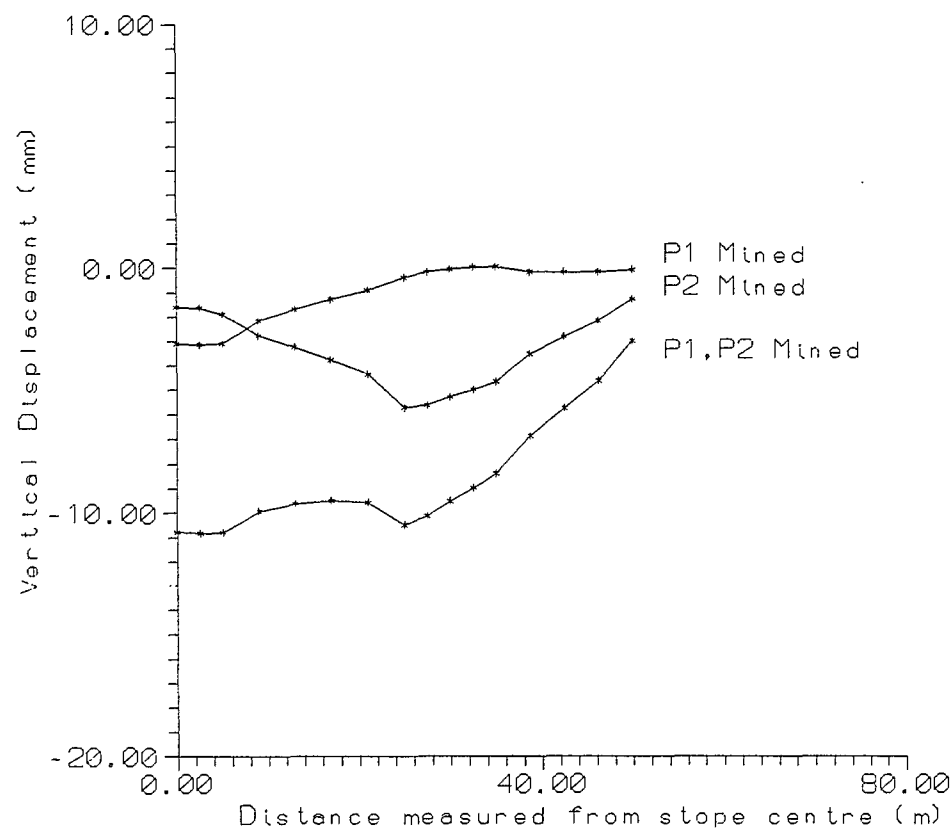


Fig. 33 - Excavation Displacements At Stope Roof, Model 3, Section 17800E

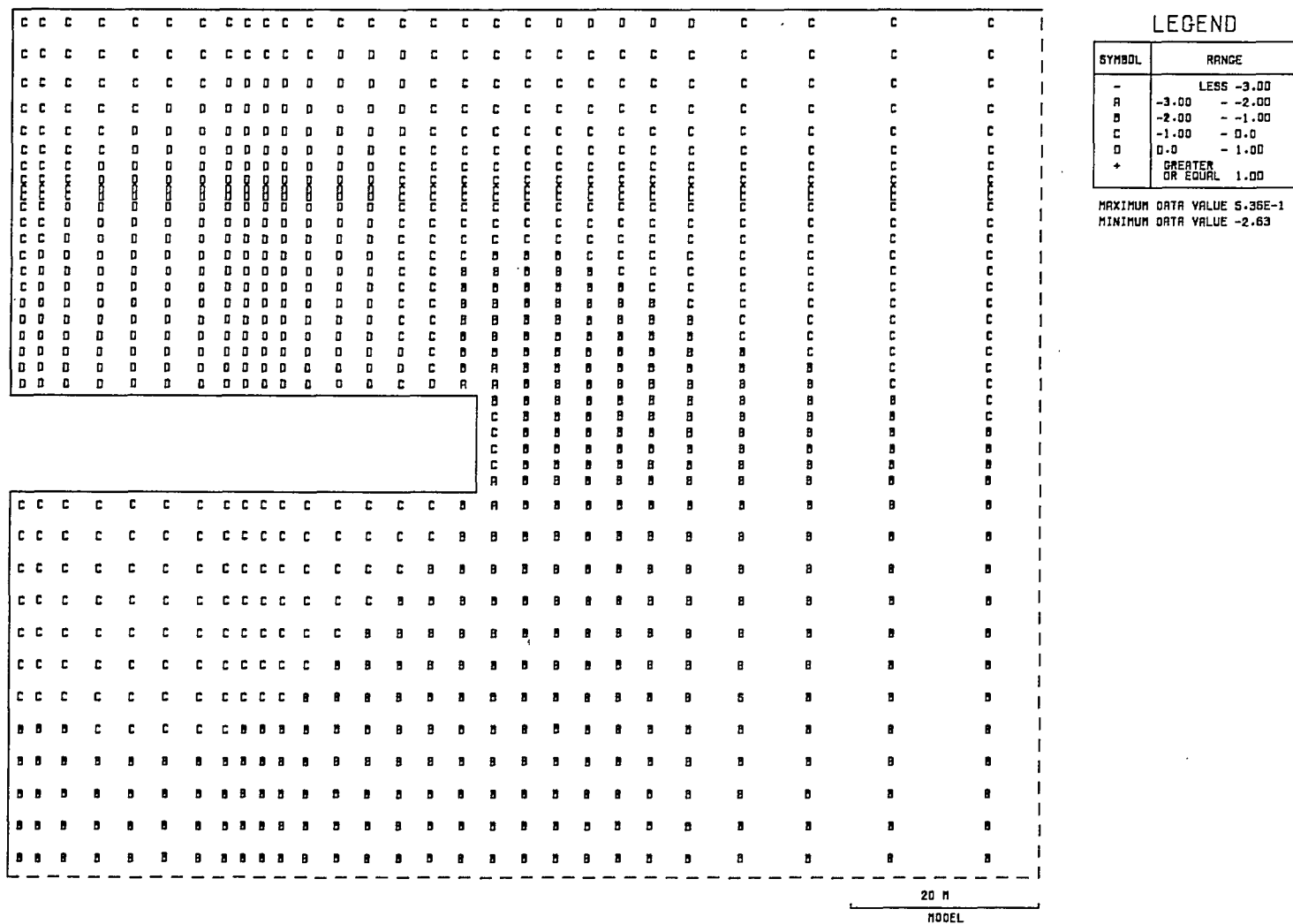
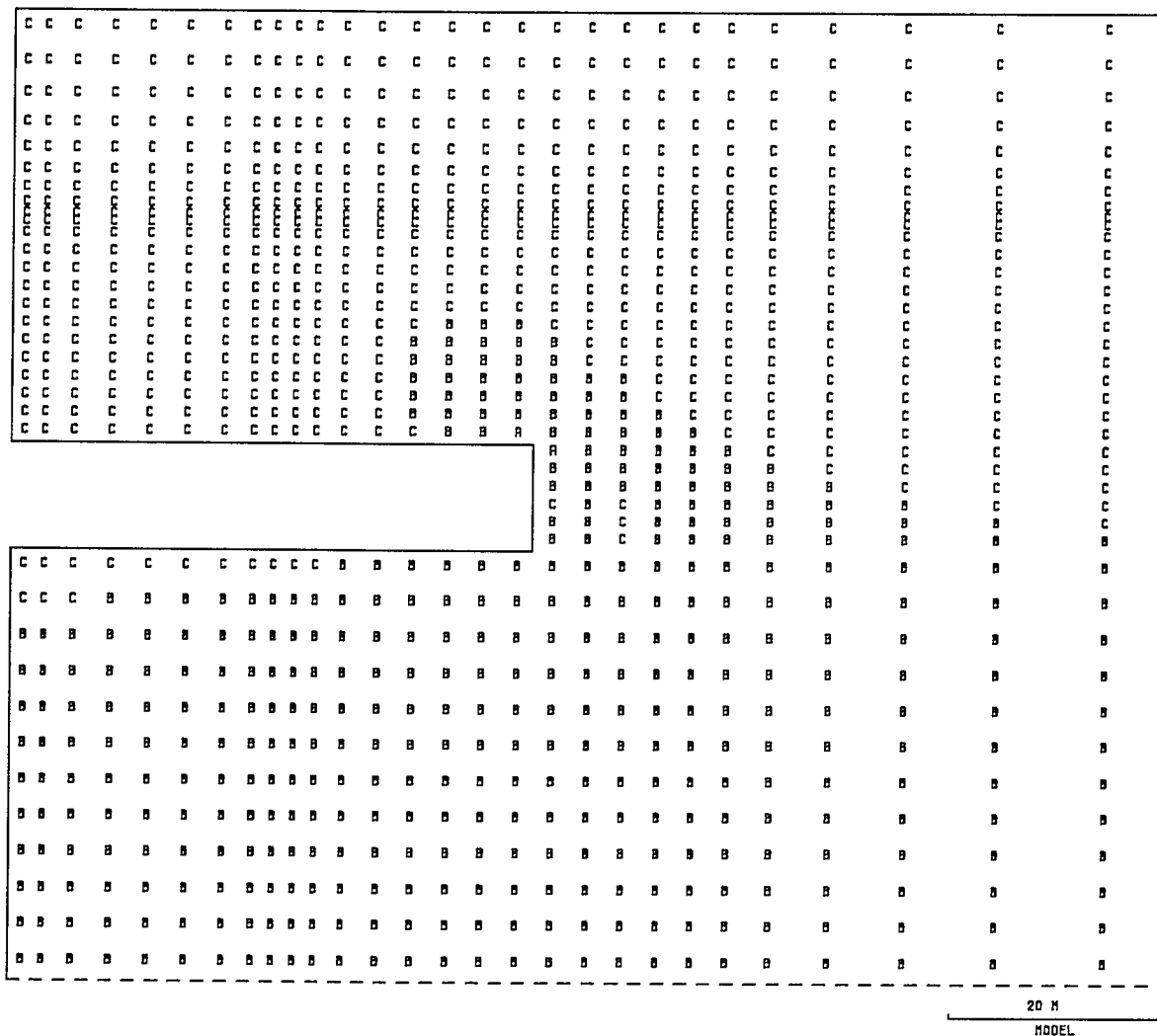


Fig. A1 - Major Principal Stress Distributions, Model 1

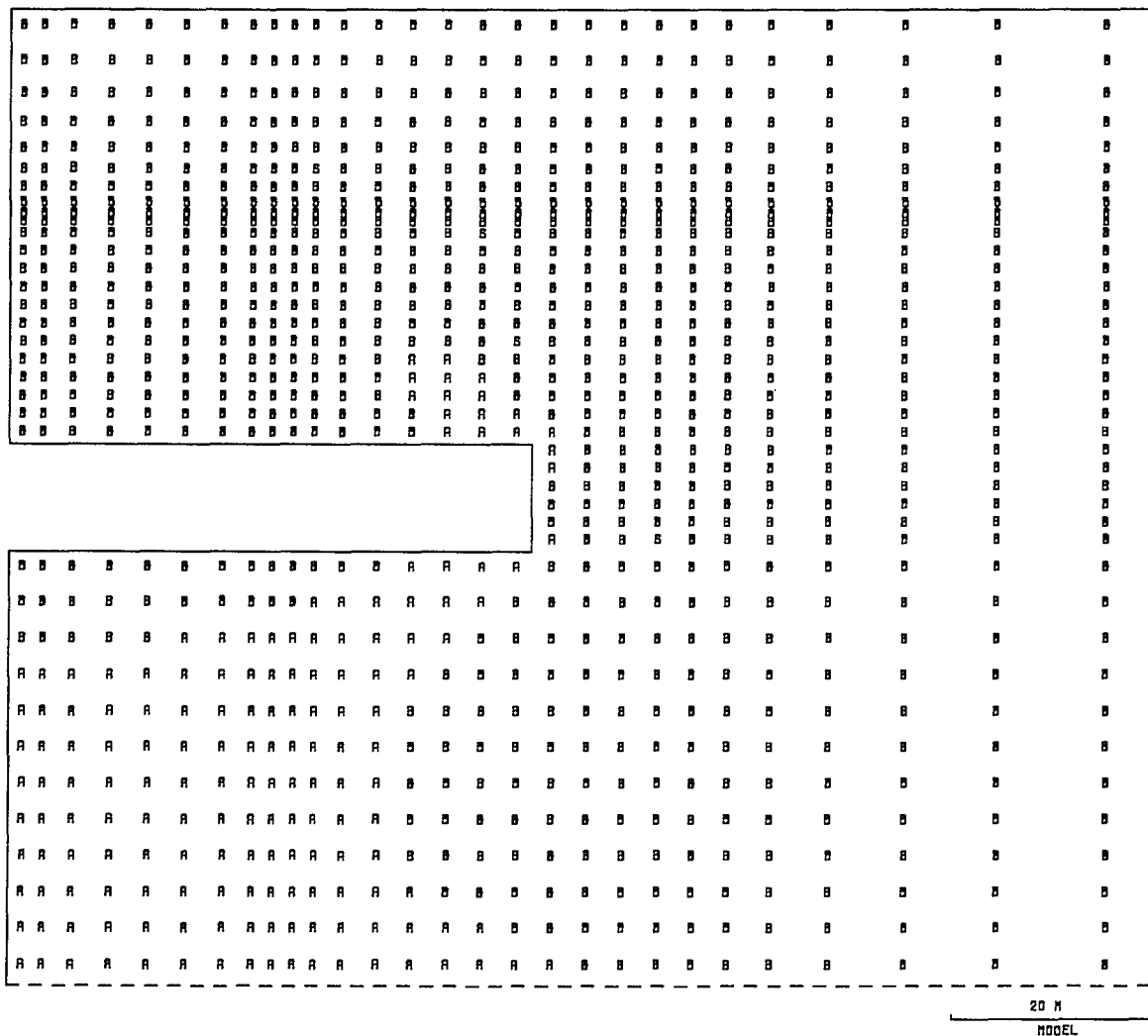


LEGEND

SYMBOL	RANGE
-	LESS -1.50E1
A	-1.50E1 - -1.00E1
B	-1.00E1 - -5.00
C	-5.00 - 0.0
+	GREATER OR EQUAL 0.0

MAXIMUM DATA VALUE -5.55E-2
MINIMUM DATA VALUE -1.28E1

Fig. A2 - Minor Principal Stress Distributions, Model 1



LEGEND

SYMBOL	RANGE
-	LESS 1.00
A	1.00 - 2.00
B	2.00 - 3.00
+	GREATER OR EQUAL 3.00

MAXIMUM ORTA VALUE 2.98
MINIMUM ORTA VALUE 1.57

Fig. A3 - Drucker-Prager Safety Factor Plots, Model 1

